

# A multiproxy-based reconstruction of the mid- to late Holocene paleoenvironment in the Laptev Sea off the Lena River Delta (Siberian Arctic)

Olga Rudenko<sup>a,\*</sup>, Ekaterina Taldenkova<sup>b</sup>, Yaroslav Ovsepyan<sup>c</sup>, Anna Stepanova<sup>d</sup>, Henning A. Bauch<sup>e</sup>

<sup>a</sup> Institute of Earth Sciences and Bioengineering, Orel State University named after I.S. Turgenev, ul. Komsomol'skaya str. 95, 302026 Orel, Russia

<sup>b</sup> Faculty of Geography, Lomonosov Moscow State University, Leninskie Gory, 1, 119991 Moscow, Russia

<sup>c</sup> Geological Institute of the Russian Academy of Sciences, Pyzhevskii per. 7, 119017 Moscow, Russia

<sup>d</sup> Texas A&M University, College Station, 77843, TX, USA,

<sup>e</sup> Alfred Wegener Institute for Polar and Marine Research, Bremerhaven c/o GEOMAR, Wischhofstr. 1-3, D-24148 Kiel, Germany

## ARTICLE INFO

### Keywords:

Pollen  
Non-pollen palynomorphs  
Foraminifers  
Ostracods  
Stable isotopes  
Holocene  
Arctic paleoenvironment

## ABSTRACT

Land-shelf interactions and related environmental changes were reconstructed for the past 6 cal. kyrs interpreting multiproxy records from the two AMS<sup>14</sup>C-dated sediment cores from the sites located to the north and northeast of the Lena River delta. Proxies used include terrestrial and aquatic palynomorphs, benthic/planktic foraminifers and ostracods paired with benthic  $\delta^{18}\text{O}$  and  $\delta^{13}\text{C}$  records of *Haynesina orbiculare*. The study focused on unravelling the relation between river runoff and the regional climate changes on the one hand, and its imprint on the shelf sea environment on timescales beyond the instrumental records on the other.

The palynomorph records show that the Lena River outflow largely determined the composition of species associations and the magnitude of terrestrial matter influx from land. Pollen assemblages of the inner Laptev Sea shelf reflect complex pollen contribution of the Arctic tundra and remote taiga zones drained by the Lena River and indicate a vegetation response to warmer-than-present climatic conditions between 6.0 and 4.5 cal. ka and a subsequent gradual cooling. Fluvial influence in the records is manifested by (1) increases in sedimentation rates; (2) high influxes of pollen/spores and freshwater chlorophycean algae, wood and plant remains; (3) negative  $\delta^{13}\text{C}$  excursions due to the introduction of dissolved inorganic carbon (DIC) from river water. Episodes of enhanced freshwater influence in the surface water layers (fluvial events) correlate with positive benthic  $\delta^{18}\text{O}$  excursions and increasing representation of river-distal species among benthics. Altogether, this points to an estuarine-like reversed (north to south) bottom current activity along the submarine paleovalleys on the shelf. The most pronounced fluvial events are recognized at 5.3–5.9, 1.5 and < 0.5 cal. ka. The oldest fluvial event coincides with the final stage of mid-Holocene climate warming. A fluvial event at 1.5 cal. ka is specifically strong at the northeastern site thus marking a direction change of the Lena River outflow at this time and the progressive protrusion of the delta. During the past 500 years distinct negative  $\delta^{13}\text{C}$  values at the northeastern site reflect enhanced riverine influence. It is therefore concluded that the unprecedented change in the  $\delta^{13}\text{C}$  trend corroborates the other evidence for a principal diversion of the major Lena River outflows into its present-day, easterly direction.

## 1. Introduction

The Arctic Ocean and its marginal seas play an important role in assessing the effects of recent global warming. Over the past decades, significant environmental changes have been recorded in many

important Arctic ecosystems such as air temperatures, sea ice cover extent and thickness, salinity fluctuations, amount and seasonality of river runoffs (Gordeev et al., 1996; ACIA, 2005 and references therein). In the Siberian Arctic, the Laptev Sea (LS) and its hinterland in particular has been identified to constitute a key region for environmental

\* Corresponding author.

E-mail addresses: [olrudenko2011@yandex.ru](mailto:olrudenko2011@yandex.ru) (O. Rudenko), [etaldenkova@mail.ru](mailto:etaldenkova@mail.ru) (E. Taldenkova), [yaovsepyan@yandex.ru](mailto:yaovsepyan@yandex.ru) (Y. Ovsepyan), [a.yu.stepanova@gmail.com](mailto:a.yu.stepanova@gmail.com) (A. Stepanova), [hbauch@geomar.de](mailto:hbauch@geomar.de) (H.A. Bauch).

<https://doi.org/10.1016/j.palaeo.2019.109502>

Received 3 April 2019; Received in revised form 29 November 2019; Accepted 30 November 2019

Available online 13 December 2019

0031-0182/ © 2019 Elsevier B.V. All rights reserved.

monitoring in terms of changing ecosystem parameters as a feedback to climate change. It has been intensively studied under the framework of the joint Russian-German collaborative “Laptev Sea System” project (Kassens et al., 1998, 2009; Kassens and Dmitrenko, 1995; ; ). Beyond monitoring the recent changes, many detailed analysis of marine sediment cores from the Laptev Sea shelf have been carried out to reconstruct changes in sedimentation regime and environment during times of post-glacial, Holocene sea-level rise which reached its highstand in the area some time during the mid-Holocene (Bauch et al., 1999, 2001a, 2001b; Bauch and Polyakova, 2000; Naidina and Bauch, 2001, 2011; Polyakova et al., 2005, 2006, 2009; Klyuvitkina and Bauch, 2006; Taldenkova et al., 2005, 2008; Razina et al., 2007; Rudenko et al., 2014).

To perspective better understand the ongoing changes in the Siberian Arctic and assess any possible future variability demands investigation of past, particularly late Holocene, environmental parameters. Among them are the spatial and temporal variability of the vast riverine freshwater outflow onto the shelf, land-ocean sediment transfer and climate-induced coastal vegetation changes. Thus, an effective approach to reconstruct such factors is to study variability in abundance and species composition of indicative fossil remains enclosed in coast-proximal marine sediments.

The aim of the study is to present new micropaleontological data from three marine sediment cores, recovered from the southeastern LS adjacent to the Lena River (LR) delta. Being the largest delta system in the entire Arctic the LR constitutes an important environmental interface today as well as in the past. We have obtained from these sites, where sediment thicknesses of Holocene age is relatively high (Bauch et al., 1999, 2001b), new data including taxonomic composition of pollen, spores and aquatic palynomorphs, assemblages of benthic foraminifers and ostracods, stable isotope composition of benthic foraminifers, together with new radiocarbon datings. The intention of this study now is to complement our new proxy records with previously published data to construct a comprehensive picture of the paleoenvironmental development over the past 6 cal kyr. The central focus will be on unravelling the relation between river runoff and the regional climate changes on the one hand, and its imprint on the shelf sea environment on timescales beyond the instrumental records on the other.

## 2. Regional setting

The Laptev Sea is a continental shelf sea of the Arctic Ocean with a gently sloping plain towards the north located between the Taimyr Peninsula in the west and the New Siberian Islands in the east. Its southern coast is dominated by the northward protruding LR, the largest delta system in the Arctic.

### 2.1. Modern oceanography and climate

The LS shelf topography reveals several submarine trough-like valleys connected to the mouths of the main rivers (Bauch et al., 1999) (Fig. 1) reflecting the last glacial low sea-level stand (Holmes and Creager, 1974; Kleiber and Niessen, 1999).

LR discharge comprises c. 70% of the total to the LS (Dmitrenko et al., 2001a). The peak values characteristic for the short summer period (Alabyan et al., 1995; Kassens et al., 1998) cause relatively low salinity in the affected shelf area. The LS influences Arctic climate and environments via extensive heat exchange with the atmosphere during the short ice-free summer and contributes to the Arctic sea ice production during winter. In winter, fast ice extends to a depth of 20–25 m to give way to a polynya system. Interaction between inner shelf and continental slope water masses is determined by activity of offshore northeastern winds (*Meteorologicheskoye I Geofisicheskoye Issledovaniya (Meteorological and Geophysical Researches)*, 2011) and fluvial runoff, which induce reversed bottom currents, that is water moving from the

outer to the inner shelf along these paleovalleys (Dmitrenko et al., 2001b).

On the inner shelf, present-day sedimentation is affected by fluvial runoff and abrasion of permafrost coasts delivering considerable amounts of sedimentary and organic matter (Bauch et al., 2001b). During the short ice-free period, and especially during the spring breakup, suspended particulate matter (SPM) discharged by the LR settles quickly in the proximity of the delta (Wegner et al., 2003). However, stronger fluvial events may form sediment layers more enriched in terrestrial material (plant and wood fragments, etc.), much further away from the LR delta (Rivera et al., 2006). Considerable amount of SPM exceeding the riverine material is additionally supplied by coastal thermoabrasion (Rachold et al., 2000).

The LR water is discharged to the LS via four major branches cutting the delta (Fig. 1). Trofimovskaya and Bykovskaya branches are directed to the northeast and east and receive 86% of the total runoff, Tumatskaya and Olenekskaya branches flowing northward and westward receive 7% of the runoff each (Schwamborn et al., 2002a, 2002b).

### 2.2. Vegetation on adjacent land as pollen source

The transfer of terrestrial material to the LS by the various processes described above also provide ample evidence of the vegetation cover in the hinterland. Scarce arctic tundra communities frame the coast of the LS (*Atlas Arktiki (Atlas of the Arctic)*, 1985; CAVM Team, 2003 Müller et al., 2010) and a cold desert community occupies the islands. Dwarf willow (*Salix arctica*, *S. polaris* and *S. reticulata*), birch (*Betula nana* subsp. *exilis*), cereals and heath (e.g. *Ledum palustre*, *Cassiope tetragona*, *Vaccinium uliginosum* and *V. vitis-idaea*) communities are widespread to the south (Perfil'eva et al., 1991). Shrubby birch and alder (*Alnus fruticosa*) occupy the low LR valley (Savelieva et al., 2013).

Woodlands with Northern larch (*Larix dahurica*) adjoin the tundra zone from the south stretching through the southern part of the LR catchment area along the LR valley up to 71°35' N (Pisarič et al., 2001) and forming an isolated forest island Ary-Mas, the northernmost in the world (Stone and Schlesinger, 1993). *Picea obovata* distribution range extends beyond the Arctic Circle (Sokolov et al., 1977). Within the Khatanga River catchment and Taimyr Peninsula its border reaches 72°15' N (Kapper, 1954). Alder (*Alnus hirsuta*) growth within the middle course of the LR (Raschke and Savelieva, 2017) is supported by locally moister and warmer environments (Alpat'ev et al., 1976).

## 3. Material and methods

The actualistic basis for our paleoreconstructions comes from our earlier studies of the composition of pollen spectra and NPP, foraminiferal and ostracodal assemblages in the surface sediments of the LS shelf and slope (Stepanova et al., 2003, 2007; Rudenko et al., 2015; Ovsepyan, 2016). These have shown a relationship between the occurrence of river-proximal indicative species on one hand, and variations in the concentrations of those microfossils best reflecting the intensity of riverine outflow of suspended organic material from the LR onto the proximal shelf on the other hand.

The studied cores and boxcore (Fig. 1) were obtained during Transdrift II (1994) and V (1998) expeditions aboard the RV “Professor Mul'tanovskii” and “Polarstern”, respectively. Core PM9482-2 (345 cm long) was collected at 27 m water depth from north of the LR delta and the confluence of the Tumatskaya branch. Core PS51/80-13 (187 cm long, 207 cm long with core catcher) and boxcore PS51/80-11 (45 cm long) are from 21 m water depth in the eastern Lena paleovalley northeast of the LR delta, close to the Trofimovskaya branch.

Core PS51/80-13 and boxcore PS51/80-11 consist of bioturbated, organic-rich gray to dark gray silty clay. Core PM9482-2 is represented by dark greenish-gray silty clay to clayey silt below 180 cm core depth. None of the cores show any noticeable erosional features.

Core chronologies are based on radiocarbon ages measured on

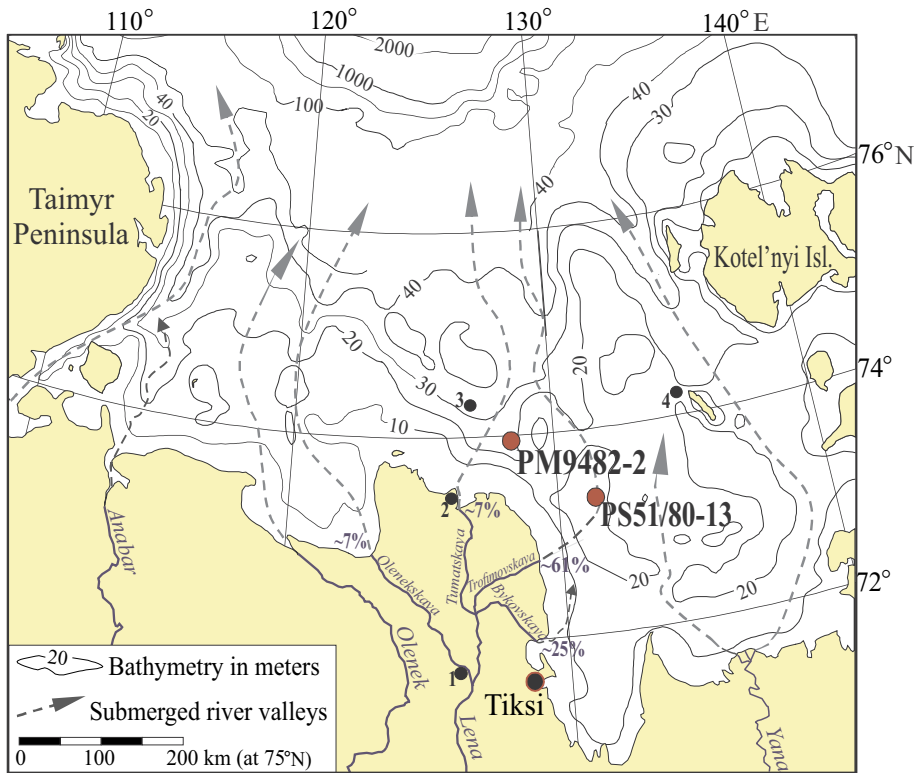


**Fig. 1.** Bathymetric map of the Laptev Sea showing submerged river paleovalleys and location of the studied cores (red dots) and the sites mentioned in the text (black dots): 1 –Lake Dolgoye (Pisarcic et al., 2001); 2 –Lake Nikolay (Andreev et al., 2004a); 3 - core PS51/092-12 ((Polyakova et al., 2006, 2009; Mueller-Lupp et al., 2004); 4 - core PM9462 (Naidina and Bauch, 2011). Note that Lake Billyakh (65°17'N, 126°47'E, Müller et al., 2009) is situated in the middle part of the Lena River region, i.e. outside the map. Olenekskaya, Tumasovskaya, Trofimovskaya and Bykovskaya branches with average freshwater discharge during “spring” are shown after Alabyan et al., 1995. (For interpretation of the references to colour in this figure legend, the reader is referred to the web version of this article.)

bivalves, mixed microfossils and a wood fragment using an accelerator mass spectrometer (AMS) at Leibniz Laboratory in Kiel (Germany). All radiocarbon dates, including those obtained previously on the two cores (Bauch and Polyakova, 2000; Bauch et al., 2001b), were converted into calendar ages with the help of Calib 7.1 program (Stuiver et al., 2017). The reservoir age of  $370 \pm 49$  years, as determined for the Laptev Sea shelf (Bauch et al., 2001b), was applied.

Vacuum-dried and weighed sediment samples from both cores were studied for pollen and spores. Samples were collected as 2 cm thick slices every 2–4 cm in core PS51/80-13 and every 5–10 cm in core PM9482-2. For the extraction of microfossils, we used centrifugal separation in potassium-cadmium ( $KJ + CdJ_2$ ) heavy liquid with a density of  $2.3 \text{ g/cm}^3$ . Prior to this, samples were processed with cold 10-% solution of HCl and 10-% solution of KOH to dissolve carbonates and silicates and then decanted with distilled water to remove clay particles. One *Lycopodium* spike tablet was added to every sediment sample prior to the chemical treatment for calculating concentrations of identified palynomorphs (Stockmarr, 1971).

Both pollen and non-pollen palynomorphs (NPP), which include freshwater colonial chlorophycean algae and marine cysts of dinoflagellates, were identified with the aid of published keys and atlases (Sokolovskaya, 1955; Kupriyanova and Aleshina, 1978; Reille, 1992; Kunz-Pirrung, 1998; Komárek and Jankovská, 2001; Savelieva et al., 2013) under  $\times 400$  magnification. In this study, *Betula* pollen is subdivided into two morphological types: *B. nana*-type (shrub birch) and *B. sect. Albae* (tree birch). *Pinus* pollen is also separated into two morphological types (*P.* subgen. *Diploxylon* and *P.* subgen. *Haploxylon*). In the study area the first pollen type is produced by *P. sylvestris* (Scots pine) and the second one is produced mainly by *P. pumila* (Siberian shrub pine) and partly by *P. sibirica* (Siberian pine), which grows in the upper LR valley.

A minimum of 160–200 pollen grains per sample were counted with exception of 9 samples, which contained  $< 150$  pollen grains. Reworked microfossils and NPP were counted in addition and their percentages were counted based on the total sum of identified microfossils. Calculation of relative pollen frequency was based on the total

pollen sum, arboreal pollen (AP) plus non-arboreal pollen (NAP). The relative pollen frequency of aquatic and nearshore plants as well as the spore percentages were calculated based on AP + NAP sum. For calculations and for drawing the percentage/concentration diagrams, we used Tilia/TiliaGraph/TGView software (Grimm, 1993, 2004). To facilitate the interpretation of palynological records along a better understanding of the relationship between the main dominants of the pollen spectra we calculated the total percentage ratio of conifers to tundra shrubs pollen (C/TSh ratio). Following the approach recently tested by palynological study in the Chukchi Sea (Kim et al., 2016), we estimated accumulation rates of terrestrial (pollen and spores) and aquatic (freshwater chlorophycean algae) palynomorphs based on grain concentrations, linear sedimentation rates between the  $^{14}\text{C}$  age points, and average Holocene wet sediment bulk density and showed them as influxes.

Fossil foraminifers and ostracods were studied only in core PS51/80-13 and boxcore PS 51/80-11; 2 cm thick samples were taken as slices, for PS51/80-13 every 10 cm and for PS51/80-11 continuously. All sediment samples were washed over a  $63 \mu\text{m}$  sieve. As the two cores were basically taken from the same site, the loss of the uppermost 30 cm in PS51/80-13 during coring was compensated for by splicing both cores together. Since sediment samples from core PS51/80-11 were washed onboard without preceding drying, the total abundance of microfossils is given versus the weight of washed sediment.

To obtain statistically meaningful results on foraminifers, relative abundance of species and ecological groups are commonly calculated only for samples which contained  $> 100$  tests (Fatela and Taborda, 2002). However, because of their scarcity in the studied core and, especially, boxcore, we used samples with  $> 50$  tests per sample. For ostracods, which are usually much less abundant, the limit for percentage calculations was set at 30 valves. This procedure is justified because samples were cut as slices that covered a rather large area.

In order to estimate biodiversity, we counted the number of species per sample and applied Shannon (H) index (Hayek and Buzas, 1997). The latter considers the abundance and homogeneity of species distribution and estimates the contribution of each species into the total

**Table 1**

AMS14C dates converted into calendar ages with Calib 7.1 program (including original datings from Bauch et al., 2001b and Bauch and Polyakova, 2000).

Lab no	Samplecm	Material	<sup>14</sup> C age, yrs BP	Calendar age, yrs BP (Calib 7.1)	$\delta^{13}\text{C}$ (‰)
Boxcore PS51/80-11 (73°27.83'N 131°39.0'E, 21 m)					
KIA 32818	2	Microfossils	955 ± 30	576 <sup>a</sup>	-8.04 ± 0.39
KIA 32819	4	Microfossils	1835 ± 30	1409 <sup>a</sup>	-10.11 ± 0.40
KIA 30106	6	Microfossils	2100 ± 35	1718 <sup>a</sup>	-9.11 ± 0.39
KIA 30107	22	<i>P. arctica</i> , microfossils	1620 ± 25	1219	-2.71 ± 0.39
KIA 30108	28	Microfossils	1645 ± 25	1240	-0.63 ± 0.40
KIA 30109	43.5	<i>Macoma</i> sp.	2240 ± 35	1879	0.40 ± 0.36
Core PS51/80-13 (73°27.56'N 131°38.3'E, 21 m)					
KIA 6873	41.5	<i>Portlandia arctica</i>	1910 ± 25	1491 (1503)	-0.52 ± 0.10
KIA 6874	71.5	<i>Portlandia arctica</i>	1940 ± 25	1529 (1522)	-2.19 ± 0.20
KIA 30110	91.5	<i>Portlandia arctica</i>	2930 ± 25	2736	1.15 ± 0.41
KIA 6875	142	<i>Portlandia arctica</i>	4795 ± 30	5127 (5097)	-0.13 ± 0.16
KIA 6876	202	<i>Portlandia arctica</i>	5950 ± 35	6388 (6393)	0.47 ± 0.25
Core PM9482-2 (74°00'N 128°11'E, 27 m)					
KIA 3128	27	<i>Portlandia arctica</i>	590 ± 30	269 (302) <sup>a</sup>	-0.04 ± 0.42
KIA 3129	47	<i>Portlandia arctica</i>	300 ± 30	0 (0) <sup>a</sup>	-1.07 ± 0.14
KIA 3130	87	<i>Portlandia arctica</i>	630 ± 30	305 (358)	0.17 ± 0.23
KIA 3131	111	<i>Portlandia arctica</i>	1190 ± 30	757 (823)	-1.73 ± 0.22
KIA 3132	161	Wood fragment	2260 ± 40	1902 (2326)	-26.00 ± 0.23
KIA 3133	241	<i>Portlandia arctica</i>	2880 ± 30	2703 (2739)	-4.14 ± 0.18
KIA 3134	273	<i>Portlandia arctica</i>	2990 ± 30	2786 (2839) <sup>a</sup>	-1.13 ± 0.27
KIA 3135	325	<i>Portlandia arctica</i>	2930 ± 40	2738 (2766)	2.08 ± 0.23

Notes: cal. age in brackets - core PS51/80-13 from Bauch et al., (2001b), core PM9482-2 from Bauch and Polyakova (2000).

<sup>a</sup> Dating excluded from age model calculation.

sum.

Composition of the stable isotopes of oxygen ( $\delta^{18}\text{O}$ ) and carbon ( $\delta^{13}\text{C}$ ) was determined on the tests of the benthic foraminifera species *Haynesina orbiculare*. This species was previously shown to be the most reliable for isotope measurements as it reflects the oxygen isotope composition of ambient water in various LS environments with a constant offset (Bauch et al., 2004). Isotope measurements were conducted at Geomar (Kiel, Germany) with the automated Kiel carbonate device coupled online to a Finnigan MAT 251 gas isotope mass spectrometer. Isotope values are reported in the usual  $\delta$ -notation relative to VPDB.

## 4. Results

### 4.1. Core chronology and sedimentation rates

The age models for core PS51/80-13 and boxcore PS51/80-11 were constructed by interpolation between the age tiepoints assuming the linear sedimentation rates between them and the modern age of core tops (Table 1). Several datings were excluded from the age model construction: the three uppermost datings of the boxcore PS51/80-11 with strongly negative  $\delta^{13}\text{C}$  signature, the two of which are reversed, and the two reversed datings from the upper and lower parts of core PM9482-2 (Table 1, Fig. 2). In the latter core, also the uppermost dating above the reversed one was omitted because of the possible influence of bioturbation.

The basal age of core PS51/80-13 is 6.4 cal. ka (with core catcher), the age of the core itself is 6.1 cal. ka (Table 1; Fig. 2). As the upper 30 cm were lost during coring, the interpolated age of the core top would be 1.1 cal. ka assuming a zero age at 0 cm. Average sedimentation rates were calculated as cm per 10–3 years (kyr) between the neighboring age tiepoints (Fig. 2). If we assume relatively constant average sedimentation rates (ASR) after 5.1 cal. ka, as has been done previously (Bauch et al., 2001b), then a significant decrease is observed after 5.1 cal. ka, from 48 to 28 cm/kyr. However, based on the additional datings ASR dropped from 48 to 21 cm/kyr between 5.1 and 2.7 cal. ka, then to 17 cm/kyr between 2.7 and 1.5 cal. ka, when a sudden and sharp increase in ASR (789 cm/kyr) occurred at around 1.5 cal. ka within < 30 years. This layer contains wood pieces and

abundant other macroplant debris. After this sudden event, ASR decreased to 28 cm/10 kyr, and that estimation could be regarded as the modern ASR for this part of the LS inner shelf. Boxcore PS51/80-11 has the basal age of 1.9 cal. ka. Until 1.2 cal. ka ASR were 25 cm/kyr that is similar to the ASR of the upper part of core PS51/80-13. Although the major ASR event at 1.5 cal. ka is not directly reflected in the boxcore sediment sequence, but there is a noticeable increase in ASR (286 cm/kyr) at 1.2 cal. ka. We assume this might also be the same event, and the age difference is due to the different material used for dating, (mollusk *P. arctica* vs. mixed microfossils).

Besides the three reversed datings from the probably highly bioturbated upper and lower sections of core PM9482-2 (Table 1; Fig. 2), it should be also noted that although the dating on wood fragment at 161 cm fits to the general trend in age, it might be several hundreds of years older than the actual age of the sediment. The extrapolated age of the core base is c. 2.8 cal. ka. ASR were extremely high, 2400 cm/kyr, in the lowermost 1 m thick part of the core dating back to 2.7–2.8 cal. ka (Fig. 2). The subsequent 1.5 m thick section was accumulated between 2.7 and 0.3 cal. ka under relatively low ASR ranging from 44 to 100 cm/kyr. During the last 300 years ASR increased up to 285 cm/kyr.

Summarizing, three short-lived events of a sharp increase in ASR were recorded in the studied cores during the last about 3 cal. kyr (Fig. 2, C): the extreme 2.7–2.8 cal. ka event in the region to the north off the LR delta; and a 1.5 cal. ka and 1.2 cal. ka events in the region to the northeast off it; the latter might be the same event given the age model and dating uncertainties. It should be also noted, that the former event at the base of core PM9482-2 might be not a short-lived event, but a continuation of a longer trend in high ASR due to the stronger influence of river runoff in the northern direction. The modern rise in ASR (0–0.3 cal.ka) observed in the northern region could not be revealed in the record of boxcore PS51/80-11 because of the reversed datings.

### 4.2. Downcore distribution pattern of pollen, spores and NPP

Ideally, the taxonomic diversity of terrestrial microfossils identified in the sediment cores should closely reflect the vegetation of the adjacent delta and hinterland. Of the total spectra 52 were pollen taxa and

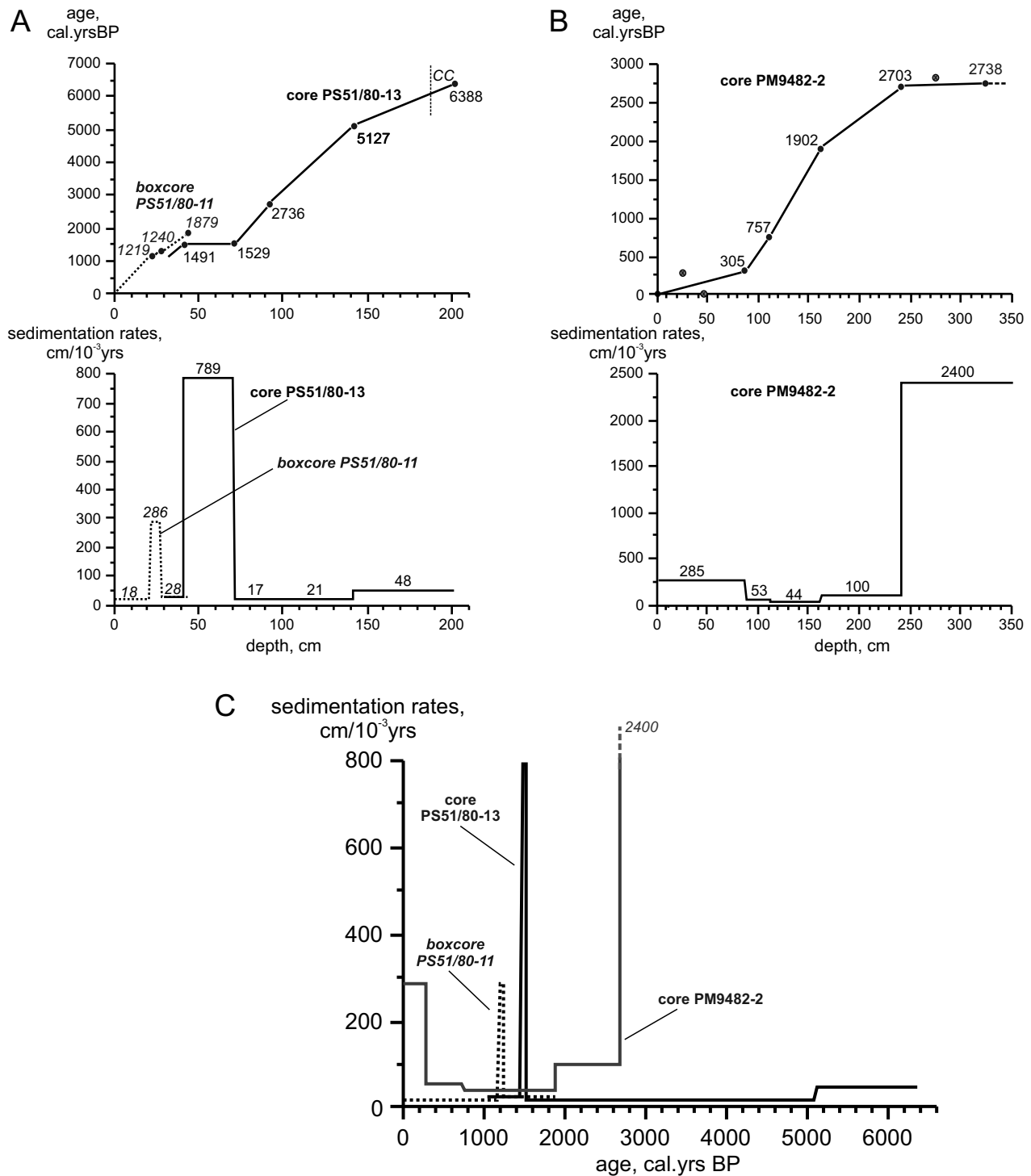


**Fig. 2.** Age-depth models and average sedimentation rates for (A) core PS51/80-13 and boxcore PS51/80-11 and (B) core PM9482-2. (C) - average sedimentation rates for all studied cores vs. calendar age. Open circles correspond to the datings that were excluded from age model construction; CC- core catcher.

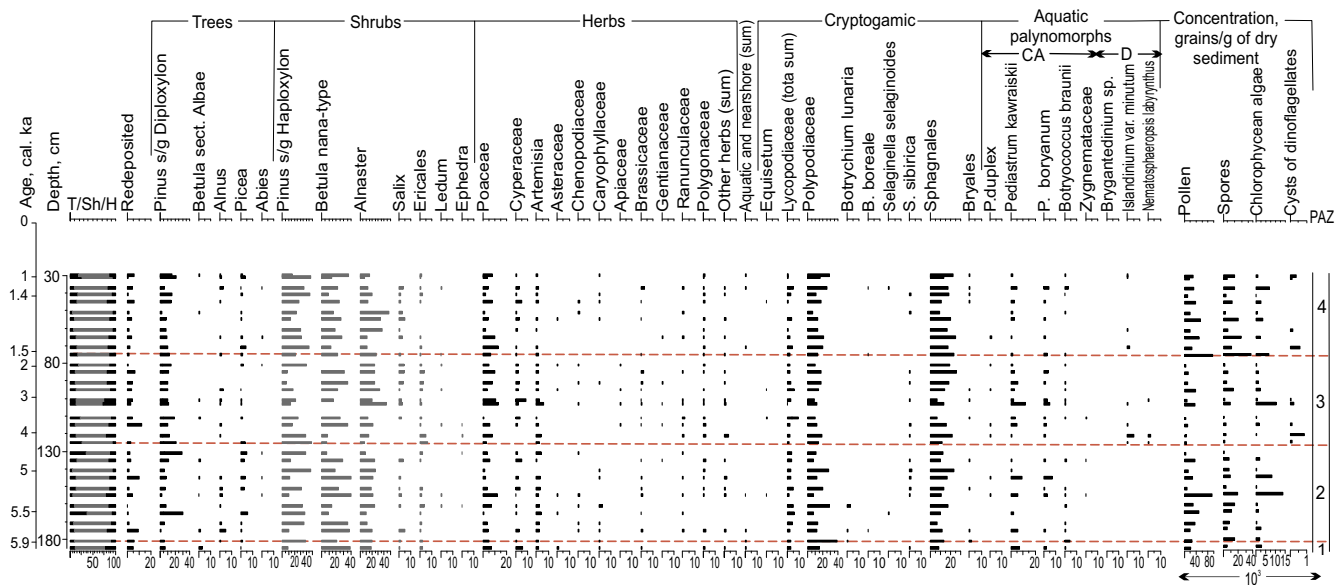
13 taxa belonged to spores of mosses and ferns, with the grassy part of the spectrum being the most diverse. The taxonomic composition of pollen and spores is overall fairly consistent throughout most of the record in both cores, while concentrations of various groups of palynomorphs change considerably, probably largely depending on the intensity of river flow and, to a lesser degree, on wind effects. Altogether they typically reflect the floristic features of several botanical and geographical zones and subzones, namely arctic wetland moss tundra, shrub tundra and taiga.

The fossil pollen spectra are dominated by pollen of shrub taxa, whose share varies from 60 to 95% being generally higher in core PM9482-2 (Fig. 3).

The enrichment of the spectra with pollen of plants typical of LR floodplain biocenoses (mainly *Alnus fruticosa* and *Betula nana*-type) and seaside low-meadow communities (*Artemisia*, Asteraceae and Chenopodiaceae) stands out as a characteristic feature of microfossil assemblage composition in both cores.

Spores of cryptogamic plants (mainly Polypodiaceae and *Shagnum*)

Core PS51/80-13



Core PM9482-2

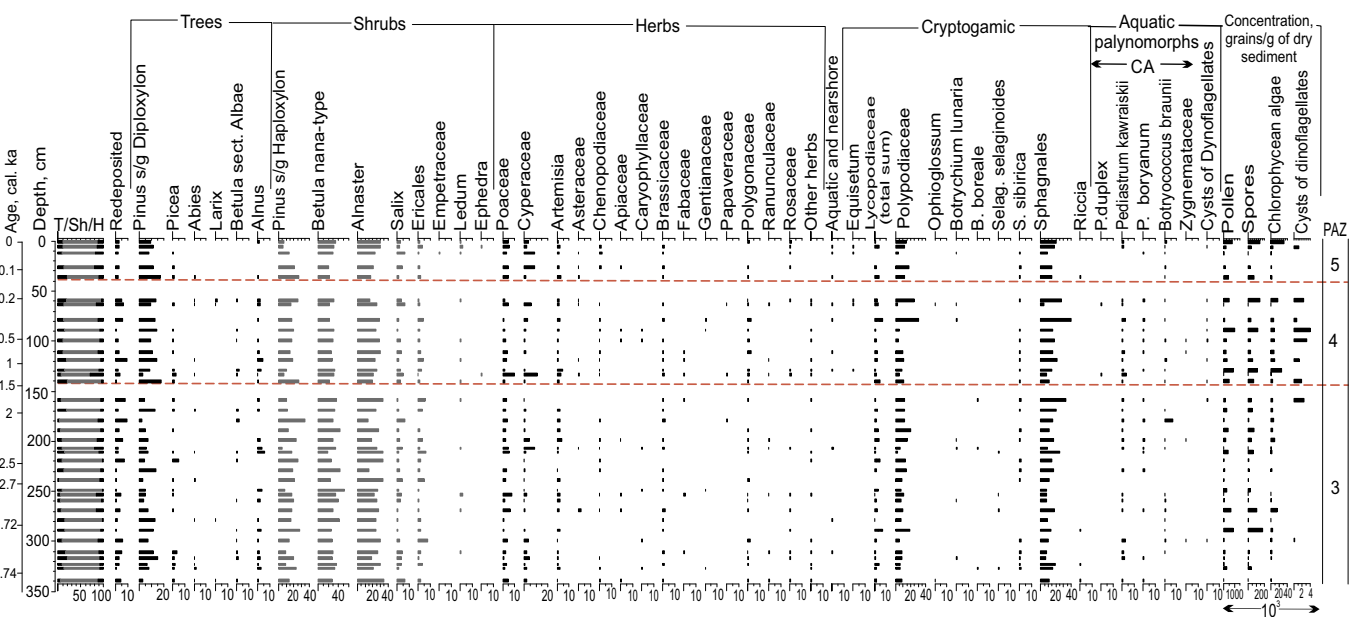


Fig. 3. Downcore distribution of pollen, spores and aquatic palynomorphs in cores PS51/80-13 and PM9482-2, %: T – pollen of trees; Sh – pollen of shrubs; H – pollen of herbs and grasses; L – pollen of *Larix dahurica*; CA – chlorophycean algae; D – cysts of dinoflagellates; PAZ – pollen assemblage zones.

predominate over the other spores. The aquatic palynomorph assemblage is represented by only 5 species of freshwater chlorophycean algae, cysts of coldwater species *Islandinium minutum* common for the freshened waters on the inner LS shelf (Kunz-Pirung, 1998; Polyakova et al., 2009) and *Brygantedinium* sp. Species *Pediastrum kawraiskii* and *P. boryanum* as well as *Botryococcus* cf. *braunii* are the most abundant among freshwater chlorophycean algae. They occur throughout both core sequences thus indicating a steady, north- and northeastward river water transfer through the Lena Delta.

The group of reworked pollen is represented mainly by Mesozoic conifers (*Piceapollenites*, *Pinuspollenites*, Taxodiaceae/Cupressaceae, *Ginkgo* sp., isolated *Podocarpus unica* Bolch.) and numerous three-prong

spores (*Gleichenia delicata* Bolch., *G. umbonata* Bolch., *G. laeta* Bolch, *G. rasilis* Bolch., *Leiotrilletes*, *Phleboteris*, isolated *Lygodium* sp.) and does not exceed 5–15% in total. Dark and crumpled pollen grains of *Betula* and *Artemisia* with thickened exine were also considered to be redeposited.

On the basis of downcore taxonomic changes in microfossil composition and abundance 5 pollen assemblage zones (PAZ) were established: 1–4 - in core PS50/80-13 and 3–5 - in core PM9482-2. Their description is combined and given below.

PAZ 1 corresponds to the lower sediment interval (180–185 cm) of core PS50/80-13 aging back to 5.9–6.0 cal. ka (Fig. 3). It is characterized by the low concentration of pollen ( $20.6 \times 10^3$  grains/g) and

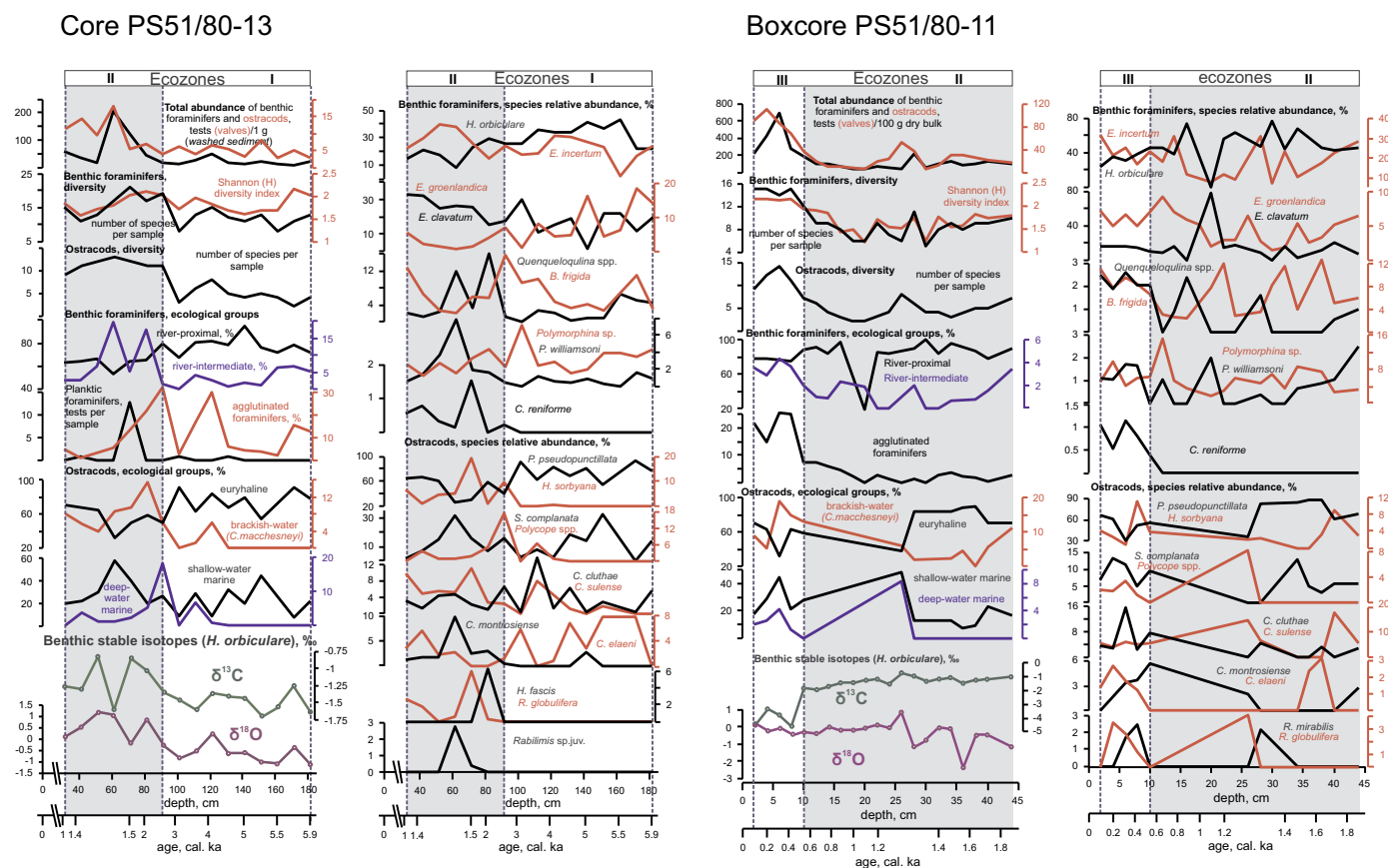


Fig. 4. Downcore distribution of foraminifers, ostracods and benthic stable isotope composition  $\delta^{18}\text{O}$  and  $\delta^{13}\text{C}$  (*Haynesina orbiculare*) in core PS51/80-13 and boxcore PS51/80-11.

chlorophycean algae remains ( $2.8 \times 10^3$  grains/g) along with the absence of cysts of dinoflagellates. Pollen of tundra shrub taxa (*Betula nana*-type and *Alnus fruticosa*) predominates reaching 18.9% and 38%, respectively. Long-distant transported *Pinus* pollen shows the lowest percentage of < 8%. In the grassy part of the spectrum, the share of pollen of Poaceae and Cyperaceae (14% in total) is rather substantial.

PAZ 2 covers the sediment interval of 127–180 cm in core PS50/80-13 corresponding in age to 4.1–5.9 cal. ka (Fig. 3). It reveals a significant increase in pollen and freshwater algae concentrations up to the highest peaks of  $94.2 \times 10^3$  and  $13.6 \times 10^3$  grains/g, respectively, at 155 cm core depth dating back to 5.3 cal. ka. A sharp increase in the content of *Pinus* pollen up to 30% at the top of the zone, as well as the appearance and growing proportion of the pollen of dark-needle conifers (*Picea obovata* and *Abies*) are the most remarkable features of the zone as well as the appearance of single *Larix dahurica* pollen.

Growing proportion of *Botrychium lunaria*, an indicative forest taxon, predominance of *Sphagnum* and Polypodiaceae spores along with a quasi-continuous presence of frost-tolerant Siberian rock-spike moss spores feature the spore assemblage.

PAZ 3 characterizes the sediment interval of 70–127 cm in core PS50/80-13 dating back to 1.5–4.2 cal. ka (Fig. 3). The interval of 145–345 cm in PM9482-2 core (Fig. 3), which corresponds in age to approximately 1.5–> 2.7 cal. ka could be correlated with the upper part of PAZ 3 in core PS50/80-13. They both reveal the highest percentages of arctic shrubs (*Alnus fruticosa*, *Salix* sp., *B. sect. Nanae*, Ericales) (up to > 85–90% in total). The lowest percentage maximum of Cyperaceae (11%) is revealed against the background of the constant presence of Poaceae in an amount of at least 10%. The other herb pollen taxa although being rich in diversity are of minor importance, except for slightly higher than in PAZ 2 share of *Artemisia*, Asteraceae and Chenopodiaceae in the lower part of the zone in core PS51/80-13.

Cysts of dinoflagellates appear in PAZ 3 at 120 cm (4.1 cal. ka) but immediately rise in concentration to peak values of up to  $8.4 \times 10^2$  grains/g of dry sediment. They are represented in this core interval by both cryophilic species *Islandinium minutum* and *Nematosphaeropsis labyrinthus*, a species which is adapted to comparatively warmer climatic conditions (Matthiessen, 1995) and demanding marine salinities above 20 (De Vernal et al., 2001).

PAZ 3 demonstrates also a significant drop in pollen concentration to the lowest values around  $8\text{--}10 \times 10^3$  grains/g on average towards the top of the zone, where then the concentration rises abruptly to a peak value exceeding  $95 \times 10^3$  grains/g in core PS51/80-13 at 80 cm aging back to 1.5 cal. ka. In core PM9482-2 the same picture could be seen at 140 cm, and pollen concentration is much higher than in core PS51/80-13. Pollen diagrams reveal similar “jumps” in the abundance of chlorophycean algae remains, particularly pronounced in core PM9482-2. Peaks in concentration of microfossils in core PS51/80-13 match with the sharp increase in ASR (789 cm/kyrs) (Fig. 2).

PAZ 4 covers the uppermost 30–70 cm interval in core PS50/80-13 corresponding to 1.1–1.5 cal. ka. Taking into account that the upper 30 cm of the core top were lost, we assume that in core PM9482-2 the correlative pollen assemblage zone covers the 40–145 cm interval accumulated during the time period of 0.3–1.5 cal. ka. A steady decrease in pollen concentration to the average values of  $11\text{--}28 \times 10^3$  grains/g in core PS51/80-13 is likely a result of the abrupt drop in ASR (Fig. 2) after 1.5 cal. ka. In core PM9482-2, despite a strong variability, pollen concentration remains slightly higher (around  $30\text{--}50 \times 10^3$  grains/g on average). Pollen of *Alnus fruticosa*, *Betula nana*-type, Poaceae and Cyperaceae dominate the spectra, though decreasing in representation in favor of both *Pinus* subgen *Diploxylon* and *P.* subgen *Haploxylon*. The percentage of the pollen of grasses and heaths also decreases slightly, amounting to 5–7% in total.

PAZ 5 is established in the topmost 40 cm interval of core PM9482-2 and corresponds to the last 0.3 cal.yrs. It mirrors the depleted proportion of conifers in favor of dwarf shrubs and Cyperaceae, suggesting an increase in pollen productivity of shrubby tundra plants.

#### 4.3. Downcore distribution pattern of foraminiferal and ostracodal assemblages

Foraminiferal assemblages in core PS51/80-13 and boxcore PS51/80-11 are dominated by “river-proximal” species quite typical for the Arctic (cf. Polyak et al., 2002a). This group makes up between 55 and 95% in the core and up to 100% in the boxcore (Fig. 4). This assemblage could be considered as a stable one, typical for this part of the sea as evidenced by the rather high, for the Arctic, Shannon diversity index (H) that varies between 1.6 and 2.1 (Patterson and Kumar, 2002; Babalola et al., 2013). “River-distal” species are absent in these inner shelf cores, the group of “river-intermediate” species (cf. Polyak et al., 2002a) averages 4–5% but reaches up to 20% in the upper part of core PS51/80-13 (Fig. 4). Along with calcareous benthic foraminifera there are also agglutinated forms as well as single tests of planktonic species *Neogloboquadrina pachyderma* sin.

Similar to foraminifera, typical inner shelf euryhaline species *Paracyprideis pseudopunctillata* and *Heterocyprideis sorbyana* dominate among ostracods in most samples (up to 92%) (Fig. 4). Brackishwater species *Cytheromorpha macchesneyi* is constantly present in the boxcore and in the upper part of the core sections. Diverse shallow-water marine species occur in all studied samples averaging about 20–30%. Relatively deep-water species, represented by *Polycope* spp., *Cytheropteron occultum* and *C. inflatum*, usually constitute < 5% in the upper 100 cm of the core and in the upper 25 cm of the boxcore. Although not shown in Fig. 4, ostracod juvenile ratio stays low throughout the record, averaging 30–50%, pointing to some degree of redeposition (Whatley, 1983).

Based on the taxonomic changes of fossil benthic assemblages three ecozones were established (Fig. 4). Ostracod juvenile ratio stays low throughout the record, averaging 30–50%, pointing to some degree of redeposition (Whatley, 1983).

*Ecozone I* corresponds to the lower sediment interval (90–183 cm) of core PS51/80-13 corresponding to 2.7–5.9 cal. ka. It is characterized by the low abundance and diversity of microfossils, predominance of “river-proximal” species among benthic foraminifera (mainly *Haynesina orbiculare* and *Elphidium incertum*) and euryhaline species *P. pseudopunctillata* among ostracods. Relatively high representation of agglutinated foraminifera (*Reophax scorpiurus*, *Ammotium cassis*, *Trochammina nana*, *Eggerella advena*, *Textularia torquata*) in combination with the low abundance of microfossils might be a result of carbonate dissolution due to diagenetic alteration of organic matter delivered to the former nearshore zone by river runoff and coastal abrasion.

*Ecozone II* characterizes the upper interval (30–90 cm) in core PS51/80-13 and the lower interval (10–45 cm) of boxcore PS51/80-11 corresponding in age to 0.5–2.7 cal.ka (Fig. 4). Fossil assemblages of this ecozone demonstrate increasing abundance and diversity of all groups of microfossils, and decreasing percentage of “river-proximal” foraminifera and euryhaline ostracods. This interval also contains more representatives of the “river-intermediate” group of foraminifera, including the relatively deep-water species *Cassidulina reniforme*. The highest number of tests (13) of planktic foraminifer *N. pachyderma* sin. per sample is recorded at the depth of 70–73 cm (1.5 cal. ka). Brackishwater ostracod species *C. macchesneyi* that was absent in the ecozone I is constantly present here. It occurs at salinities above 18 (Frenzel et al., 2010), while *P. pseudopunctillata* and *H. sorbyana* tolerate salinities as low as 5. Other ecological groups of ostracods, shallow-water as well as deep-water marine ostracods increase in abundance within this ecozone reflecting salinity increase.

Also, the share of opportunistic foraminiferal species *Elphidium clavatum* is rather high. It is possible to assume that this could be a

result of climate cooling and more severe sea-ice conditions. Such conditions are favourable for *E. clavatum*.

*Ecozone III* from the uppermost 10 cm in boxcore PS51/80-11 corresponds to the last 0.5 cal. kyrs (Fig. 4). The total abundance and diversity of benthic microfossils is high. Marine influence in the bottom water layer is strong as evidenced by the growing proportion of “river-intermediate” foraminifera, shallow-water and deep-water ostracods. Numerous agglutinated foraminifera are represented by *R. scorpiurus*, *A. cassis*, *Thurammina favosa*.

#### 4.4. $\delta^{18}\text{O}$ and $\delta^{13}\text{C}$ records of *Haynesina orbiculare*

Between 5.9 and 2.7 cal. ka, the  $\delta^{18}\text{O}$  record of core PS51/80-13 shows generally low values with a clear upward trend to more heavy values, from  $-1.1$  to about  $0\text{‰}$  (Figs. 4, 6). Two episodes of heavier  $\delta^{18}\text{O}$  values, i.e. penetration of more salty marine water, are recorded at about 5.6–5.9 cal. ka and 4.0–4.3 cal. ka. Carbon isotopic composition  $\delta^{13}\text{C}$  shows little variability remaining close to  $-1.5\text{‰}$ , but with slight positive shifts simultaneous to heavier  $\delta^{18}\text{O}$  values.

After 2.7 cal. ka,  $\delta^{18}\text{O}$  and  $\delta^{13}\text{C}$  records become more variable with generally increasing values. Oxygen isotope composition varies around  $0\text{‰}$ , but there are also short episodes of sharp positive and negative shifts. A small positive excursion is recorded at about 2.0–2.3 cal. ka, but the most pronounced positive shifts are recorded at 1.5 cal. ka (up to  $1.2\text{‰}$ ) in the core and at 1.2 cal. ka (up to  $0.9\text{‰}$ ) in the boxcore. Both episodes are preceded by negative  $\delta^{18}\text{O}$  shifts that are very low in the boxcore,  $-2.3$  and  $-1.1\text{‰}$ , whereas in the core only the older negative peak is expressed, but it is much smaller,  $-0.14\text{‰}$ . Unlike differences in  $\delta^{18}\text{O}$  values in the core and boxcore records,  $\delta^{13}\text{C}$  values are relatively the same. Small negative shifts of  $\delta^{13}\text{C}$  down to  $-1.6$ – $1.75\text{‰}$  correspond to positive  $\delta^{18}\text{O}$  shifts at approximately 1.5 and 1.2 cal. ka and likely give evidence for the riverine water input.

The most striking change in the  $\delta^{13}\text{C}$  record of the boxcore occurs since about 0.5 cal. ka (Figs. 4, 6). The values get progressively negative down to  $-4.6\text{‰}$ . This decreasing trend continues to the modern times as evidenced by the  $\delta^{13}\text{C}$  composition of *H. orbiculare* tests from the surface sample at the same locality which reveals an average value of  $-6.6\text{‰}$  (Fig. 6; Bauch et al., 2004). Oxygen isotope values are considerably less variable, but the modern  $\delta^{18}\text{O}$  of *H. orbiculare* from the surface sample is also low and averages  $-0.47\text{‰}$ .

## 5. Discussion

### 5.1. Interpretation of pollen signals from the southeastern inner LS shelf in relation to vegetation and climatic changes in the LS region and the river runoff variations

In this section we place the pollen data obtained from the LR affected LS inner shelf in a regional context by comparing them to other pollen records from marine sediment cores (Naidina and Bauch, 2001, 2011; Razina et al., 2007) as well as from coastal lakes (Andreev et al., 2004a, 2004b; Pisaric et al., 2001) and the LR catchment (Müller et al., 2009; 2010). Besides their climatological implications the marine pollen data should also provide information of river runoff variations. Assuming the estimated palynomorph concentration and influx of terrestrial palynomorphs as bioindicators of the intensity of the suspended organic matter discharge onto the shelf the revealed “freshwater” events seen in the pollen spectra can thus be compared with similar proxy records, e.g., diatoms and aquatic palynomorphs, studied on the same cores (Bauch and Polyakova, 2000; Polyakova et al., 2006, 2009).

While pollen signals from marine sediments render information on the vegetational changes on the adjacent land, they are also the result of atmospheric circulation and hydrological-erosional-preservational peculiarities. To overcome fuzziness in their interpretation we therefore used C/TSh pollen ratio between conifers and tundra plants (see Chapter 3 for details). Besides, we also took into account the changes/

relationships between ecologically heterogeneous groups of palynomorphs – terrestrial (pollen and spores), marine (cysts of dinoflagellates) and freshwater (colonial chlorophycean algae remains). A freshwater to marine palynomorph ratio, also known as a CD-index (e.g., Matthiessen et al., 2000; Polyakova et al., 2005; Gusev et al., 2014), is an effective proxy for reconstructing paleohydrological environments. As we applied heavy liquid separation for palynomorph extraction, we could not use the mentioned proxy, because cysts of dinoflagellates may have been partially destroyed by such an aggressive method. Noteworthy is that our data feature a much greater amount of chlorophycean remains than was reported previously (Polyakova et al., 2006, 2009) for which we do not have a plausible explanation yet.

#### 5.1.1. The period from 6.0 to 4.5 cal. ka (mid-Holocene)

High abundance of pollen of arboreal plants is the prominent feature of mid-Holocene pollen spectra from the northern Central Siberia. That could be seen from pollen records of the LS inner shelf (this study; Naidina and Bauch, 2001; Razina et al., 2007), different parts of the East Siberia (Andreev and Tarasov, 2007; Andreev et al., 2011 and references therein; Velichko et al., 1997) as well as in the regions along the Lena River valley (e.g. Pisaric et al., 2001; Müller et al., 2009; 2010). Our pollen spectra from core PS51/80-13 reveal a striking similarity to the record from Dolgoe Lake located about 50 km upstream, on the western bank of the LR (Fig. 1; Pisaric et al., 2001). This fact points to a decisive role of river discharge in transporting terrestrial palynomorphs onto the shelf. Indeed, both marine and lacustrine records show similar percentages of the dominant arboreal taxa with shrub birch and shrub alder among them. At the same time, by contrast to the Dolgoe Lake data, PS51/80-13 pollen record reveals a much greater representation of *Pinus* subgen *Diploxylon* pollen. The latter culminates at 30% between 5.5 and 4.5 cal. ka along with an increase in the amount of *Picea* sp. and the appearance of single pollen grains of northern larch (*Larix dahurica*). These characteristic features of core PS51/80-13 record coupled with the presence of these taxa in the stomata record of Dolgoe Lake (Pisaric et al., 2001) manifest the far northward advance of forests, together with enhanced pollen productivity of conifers due to warmer-than-present climate by the end of the Holocene optimum. Most likely, forests were able to penetrate close to the LS coast along the river valleys due to milder and, perhaps, wetter local environments protected from harsh winds (MacDonald et al., 2000). Indeed, pollen and chironomid-inferred quantitative BMA (best modern analogue) reconstructions from Nikolay Lake, the largest body of water within the LR delta located at the northwestern part of Arga Island (Fig. 1; Andreev et al., 2004a), suggest mean July temperatures up to 2 °C warmer than modern ones for this time (Fig. 5).

The steep increase of conifer pollen since c. 7.5 cal. ka up to a peak values at around 40% at 5.5 cal. ka was also recorded in the sediment core from the Yana River paleovalley around 200 km to the northeast from core site PS51/80-13 (Naidina and Bauch, 2011) suggesting that a climatically-controlled influx of conifer pollen to the LS inner shelf was ubiquitous, at least within its southeastern part which has a tremendous influence of riverine water flow. Rare palynologic data from the western part of the outer shelf of the LS indicates a consistent share of conifers at about 40% (Razina et al., 2007). According to models derived from pollen records, forest expansion in northern Siberia could also be associated with an increase in precipitation due to sea level rise (Monserud et al., 1998; Kerwin et al., 1999; Wolfe et al., 2000) in conjunction with an orbitally-induced enhancement in winter insolation (Andreev and Tarasov, 2007).

Along with the elevated C/TSh ratio and terrestrial influx (Fig. 5), the pollen record of core PS51/80-13 reveals the highest species diversity in both herbaceous and spore parts of the spectra at 5.3–5.5 cal. ka, pointing to a coeval increase in pollen productivity of arctic tundra coastal plant communities which can also be interpreted as a signal of milder climatic conditions. Besides, the growing proportion of conifers and, therefore, the C/TSh ratio (Fig. 5) along with simultaneous decline

in the relative abundance of local herbs, most likely reflects the ongoing deepening of basin and retreat of coastline from the core site. Shelf flooding accompanied by active bottom abrasion may be the cause of a greater, albeit variable, amount of reworked microfossils in core PS51/80-13 in the interval corresponding to transition from PAZ 2 to PAZ 3 (~4 cal. ka.)

The relatively high sedimentation rates that persisted from 6.3 to 5.1 cal. ka occurred when site PS51/80-13 was still nearer the paleo-coastline (Bauch et al., 2001b). The massive fivefold increase in concentration and influxes of terrestrial microfossils at around 5.5 cal. ka documents a freshwater event that seems time-coeval with diatom-based paleosalinity data from the same core as well as from core PS51/92-12 (Fig. 1; Polyakova et al., 2006, 2009). Probably being climatically induced, such peaks, like the one at 5.5 cal. ka, might manifest a particularly strong influx of organic matter via the LR, which had a widespread impact down to the continental slope of the Laptev Sea (Rudenko et al., 2014). Albeit percentage curves of main pollen dominants in core PS51/80-13 do not fully resemble those of the Billyakh Lake pollen diagram (Müller et al., 2009; 2010) due to the features inherent to marine spectra, it appears that pollen records from the LS reflect rather well the supra-regional climatic fluctuations that occurred in the boreal (taiga) zone.

#### 5.1.2. Late Holocene period (4.5 cal. ka to present)

Climatologically, the most prominent feature of the Subboreal period in Siberian Arctic was, besides some general instability, a pronounced cooling since 4.5 cal. ka. This cooling trend is revealed by pollen and chironomid-inferred reconstructions from Lake Nikolay (Andreev et al., 2004a) as well as by other palynological and oxygen isotope data from Siberian Arctic (Meyer et al., 2015; Opel et al., 2011). The time-coeval pollen spectra from the LR affected inner LS shelf area corroborate these reconstructions showing a decrease in the influx and concentration of palynomorphs and a relative decrease in conifer and tundra shrubs pollen at the expense of grasses. On Taymyr Peninsula, the cooling is manifested by the decline of trees, including *Picea* (Andreev et al., 2004b). As a result of the cooling that led to forest retreat in the LS region (MacDonald et al., 2000) both river and wind governed transfer of arboreal pollen onto the shelf became significantly limited. Judging alone from the pollen in both studied cores, this general decline became particularly pronounced since 1.5 cal. ka. Simultaneously, moss-sedge-grass arctic tundra communities advanced onto the LS coast. Since then overall conditions on land remained relatively stable.

The pollen record from core PM9482-2 manifests a relatively stable and cool environment for the last 2.8 cal. kyr and the persistent river runoff interpreted from it is similar to the published one based on freshwater diatoms (Bauch and Polyakova, 2000; Polyakova et al., 2006, 2009). These two proxies evidence an enhanced fluvial influence upon the site since c. 1.5 cal. ka, which is reflected by generally increasing, though variable, values of pollen and freshwater chlorophycean algae concentrations (Fig. 5). Both values are more than an order of magnitude higher in core PM9482-2 than in core PS51/80-13 likely due to a somewhat closer location to the coast. Besides a peak in C/TSh ratio in core PM9482-2 at 2.7–2.8 cal. ka that might indicate the considerable flow of the LR runoff in the northern direction prior to 2.7 cal. ka, the generally low C/Tsh values prior to 2.2 cal. ka were probably due to climate cooling. The drastic increase in the influx of terrestrial palynomorphs and chlorophycean algae in core PS51/80-13 at around 1.5 cal. ka certainly mirrors a strong fluvial event which is correlative with a warming reconstructed from chironomid records in Lake Nikolay (Fig. 5). However, in core PM9482-2, a significant increase in pollen and algae concentrations together with a slight increase in influxes are evident at around 1.1–1.2 cal. ka, time-coeval with a fluvial event recorded in boxcore PS51/80-11 (Fig. 6). It is difficult to judge whether the 1.2 and the 1.5 fluvial events represent a single event or these were two different events (see Sections 4.1, 4.2 and 5.2 for

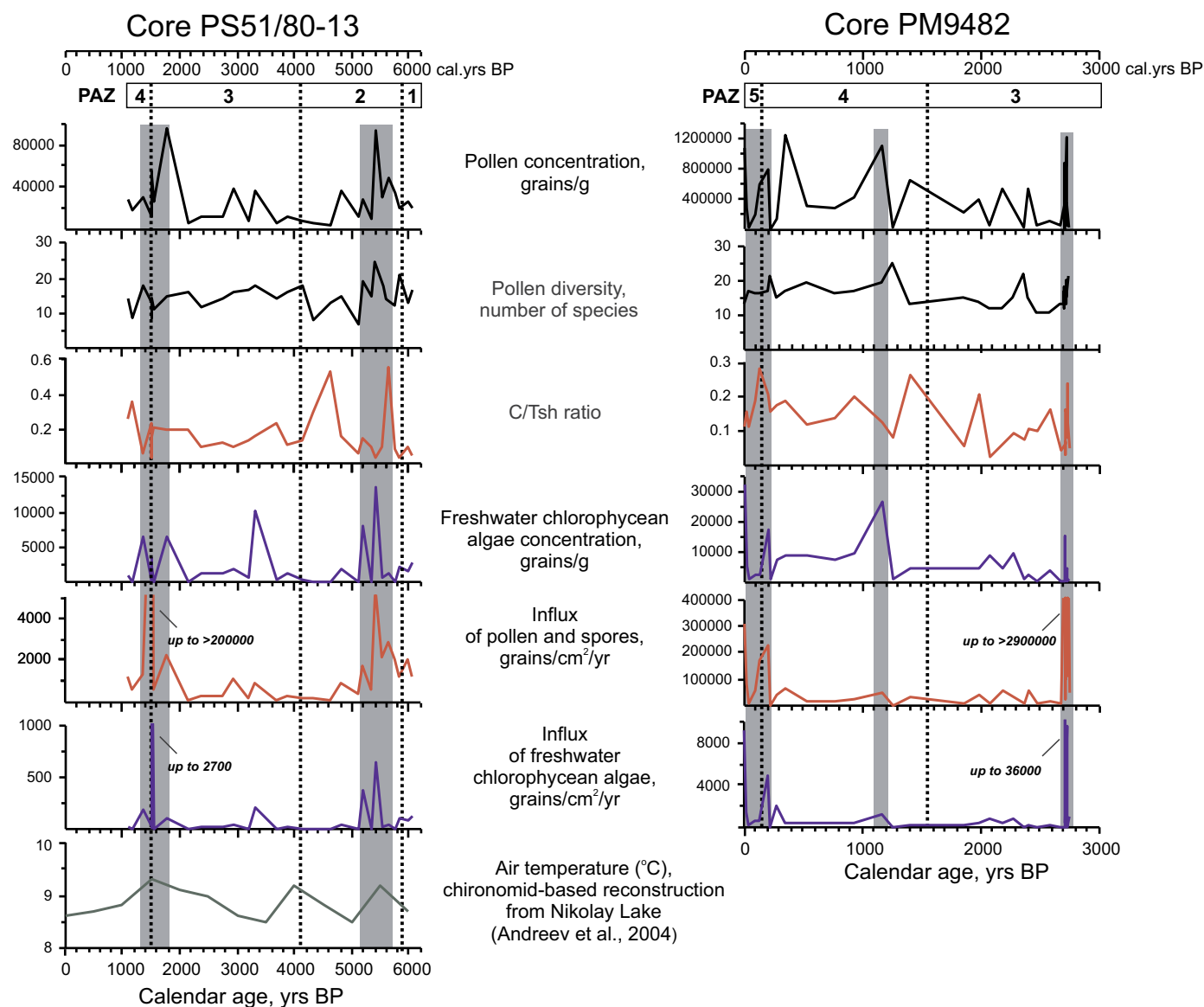


Fig. 5. Palynomorph proxies for cores PS51/80-13 and PM9482-2 along with chironomid-inferred mean July temperature paleorecord for the Lena Delta region (Andreev et al., 2004a, 2004b). Gray shading highlights episodes of high influxes of terrestrial organic matter onto the shelf related to increased fluvial influence.

discussion).

Palynomorph data of the uppermost 20 cm of core PM9482-2 are somewhat conflicting and harder to explain. The sharply rising concentration of pollen and freshwater chlorophycean algae indicates enhanced fluvial input, but contradicts the decreasing concentration of freshwater diatoms and rising percentage of sea-ice species as reported in Bauch and Polyakova (2000). According to the established relationship between the proportions of different ecological groups of diatoms in the LS surface sediments (Bauch and Polyakova, 2000), this suggests that due to continuing coastline retreat the location of the core site PM9482-2 likely shifted from a nearshore zone under the winter fast ice cover to its modern position within the more distal offshore region with seasonal polynya and drift ice cover. Another puzzling issue is the contrast in the concentration of chlorophycean algae in our record and in Polyakova et al. (2006). Regardless of these unsolved problems, based on palynomorphs we can assume that freshwater influence upon PM9482-2 was always relatively high. The more recent freshwater events might have been facilitated by climatic warming as reconstructed from compiled circumpolar paleoclimatic records. These show that over the past five centuries the last 150 years were the

warmest in the Arctic (Overpeck et al., 1997), a warming that led to increased river runoff around the Arctic (Peterson et al., 2002; Wagner et al., 2011).

## 5.2. Fluvial events and their manifestation in bottom water environment

Taxonomic changes in fossil microfaunal assemblages from river-proximal to more marine ones and the variations in isotopic composition of benthic foraminifers from core and boxcore PS51/80 reveal the combination of three major aspects of the local paleoenvironmental variability during the last 6 cal. kyr under the modern-like sea-level position (Bauch et al., 2001b): (1) the gradual increase in water depth and water stratification; (2) the growth and offshore protrusion of the LR delta; and (3) the coupling between enhanced river outflow influence in the surface water layer and activation of reversed bottom currents - from north to south - within the LR paleovalley on the inner shelf, i.e. estuarine-like circulation (Fig. 6).

This type of circulation, which is largely wind-forced, controls hydrology and sedimentation on the inner- and central LS shelf (Dmitrenko et al., 2001b; Wegner et al., 2003, 2005; Pivovarov et al.,

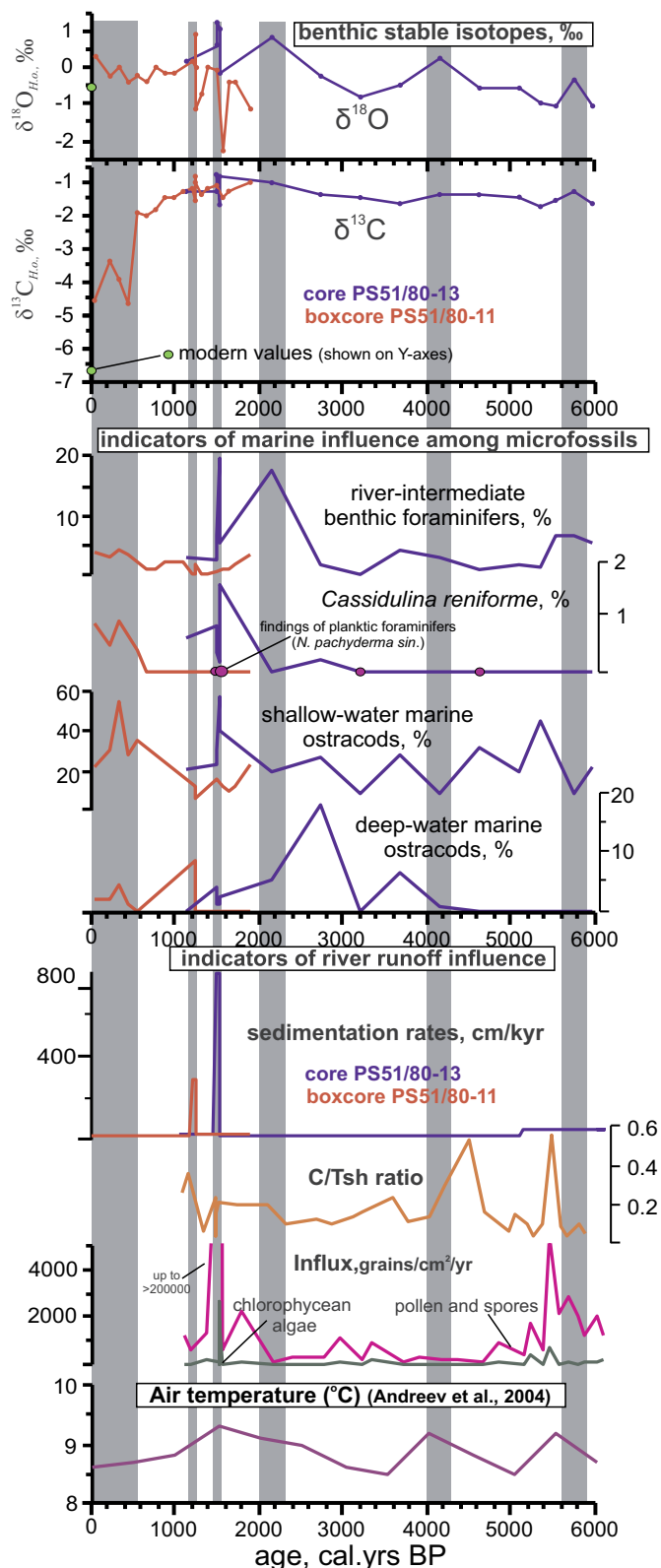


**Fig. 6.** Sedimentation rates, isotopic and microfossil records of site PS51/80 together with the chironomid-inferred mean July temperature paleorecord (Andreev et al., 2004a). Gray shading highlights episodes of increased marine influence of reversed currents in the bottom water layer. Modern  $\delta^{18}\text{O}$  and  $\delta^{13}\text{C}$  values of *Haynesina orbiculare* (Rose Bengal stained) from surface sediment sample at the same location are taken from Bauch et al., 2004. (For interpretation of the references to colour in this figure legend, the reader is referred to the web version of this article.)

2005). As the LR runoff is strongly seasonal with its peak occurring in early summer (Ivanov and Piskun, 1999; Alabyan et al., 1995; Kassens et al., 1998), the huge input of freshwater during floods could also trigger reversed bottom current flows. In the nearshore region around the LR delta extremely strong flood events may form fluvial sandy layers with eroded lower boundary, and inclusions of terrestrial plant material and wood fragments that can be traced 30–40 km offshore (Rivera et al., 2006). At these river-proximal sites high accumulation rates result in thick high-resolution sediment sequences with fluvial layers intercalating with fine-grained marine layers (Rivera et al., 2006). At the more distal localities, like the studied PS51/80 site, direct evidence of fluvial bedload layers is not present, but here one can find indications of the influence of open-sea waters reaching the inner LS shelf along the LR paleovalley. They are manifested by positive  $\delta^{18}\text{O}$  shifts and the increase in the percentage of the relatively deep-water marine species (including planktic foraminifers) at the expense of the typical inner shelf ones. We have distinguished 6 such intervals (or 5 if considering the events at 1.5 and 1.2 cal. ka to be the same event, see Section 4.1) (Fig. 6).

The two oldest intervals, dated to 5.6–5.9 and 4.0–4.3 cal. ka, occurred during the times when the core site was located in a shallow nearshore environment as indicated by generally low  $\delta^{18}\text{O}$  values and the predominance of river-proximal benthic species (Ecozone I). Mixing of fresh LR water with  $\delta^{18}\text{O}$  of  $-18.8\text{‰}$  and saline open-sea water with  $\delta^{18}\text{O}$  of  $0\text{‰}$  primarily determines the  $\delta^{18}\text{O}$  composition of bottom waters and corresponding equilibrium calcite (Bauch et al., 2004). Bottom waters in the river-affected Arctic shelf seas gain the  $0\text{‰}$  signature at salinity around 30 psu that is usually attained at water depths around 20 m (Polyak et al., 2003). At smaller depths, mixing with riverine water is active, and the  $\delta^{18}\text{O}$  composition of bottom water is negative. The calculated equilibrium calcite  $\delta^{18}\text{O}$  for the studied site PS51/80 demonstrates seasonal variability, and ranges from  $-1.9\text{‰}$  to  $-1.0\text{‰}$  in summer and from  $-3.5\text{‰}$  to  $-1.0\text{‰}$  in winter (Bauch et al., 2004). Interestingly, this seasonal difference might be also regarded as an indication of enhanced reversed bottom currents in summer due to both, wind action over ice-free sea and early summer flood. Given the constant positive offset from equilibrium calcite in *H. orbiculare* that equals  $1.7\text{‰}$  (Bauch et al., 2004), the observed range of  $-0.5$  to  $-1\text{‰}$  prior to 3–2.7 cal. ka implies  $\delta^{18}\text{O}$  of bottom waters was around  $-2.5\text{‰}$  due to the strong mixing in the nearshore zone with water depths  $< 15\text{--}20$  m. Composition of benthic microfossil assemblages also gives evidence for a shallow nearshore environment. The dominant species among foraminifers are *H. orbiculare* and *E. incertum* that are typical of nearshore regions including the outer estuaries of the Yenissei and Ob' rivers (Polyak et al., 2002a). The same is true for the dominant ostracod euryhaline species *P. pseudopunctillata* (Stepanova et al., 2003, 2007). Altogether this is a manifestation of a relatively shallow-water environment, where stratification of the water column was frequently distorted by winds, tides and downward penetration of river flood waters. Although Holocene sea-level was already at its modern height (Bauch et al., 2001b), the regional topography was still different. The coast was closer to the core site, given the average rates of coastal retreat due to thermal abrasion of 2–6 m/year during the late Holocene (Are, 1980). The present-day submarine shoals located east from the core site were exposed and formed large islands, the last remnants of these former islands disappeared only in the 20th century (Klyuev et al., 1981). Due to this proximity to actively abraded coasts, ASR remained relatively high (48 cm/kyr) until about 5 cal. ka, and then progressively decreased to 21–17 cm/kyr thereafter.

At the same time, the LR delta was less protruded offshore; its youngest eastern sector represented by the fluvial first terrace only started to accumulate around 5–6 cal. ka, and since then the delta expanded by 120–150 km mainly in northeastern and eastern directions (Korotaev, 1984, 2011; Are and Reimnitz, 2000; Schwaborn et al., 2002a). Although the LR mouth was farther from the site, the influence of river runoff was strong. The increases in the influxes of terrestrial

palynomorphs and chlorophycean algae as well as in the C/Tsh ratio at 5.4–6 cal. ka generally tend to correlate to the positive  $\delta^{18}\text{O}$  excursion and the rise in the proportion of river-intermediate benthic foraminifers, thus giving evidence for enhanced fluvial influence and reversed current activity (Fig. 6). The certain observed offsets could be related to the active coastal degradation on the one hand, or to changes in atmospheric circulation on the other. The latter can also induce reversed bottom water counter flows in the shallow inner shelf zone. However, for the same time interval, surface water salinity reconstructions based on the concentration of freshwater diatoms suggest freshening below 13 psu at the site PS51/80 as well as the site PS51/92 located farther north along the LR paleovalley (Polyakova et al., 2006). This enhanced freshwater influence correlates with climate warming as recorded not only by our palynomorph data, but also by chironomid-based paleotemperature reconstructions (Andreev et al., 2004a; Fig. 5). The less expressed fluvial event of 4.0–4.3 cal. ka also correlates with rising air temperatures (Fig. 6).

After about 2.7 cal. ka,  $\delta^{18}\text{O}$  becomes generally heavier, close to or above 0‰ (excluding the negative offsets in the boxcore, Fig. 6), although being still lower than the  $\delta^{18}\text{O}$  signature of the normal marine bottom water. Together with the growing total abundance, taxonomic diversity and proportion of marine species among benthic microfossils increase (Ecozones II and III) thus pointing to water deepening and coastline retreat. The latter is confirmed by the generally low ASR of 25–28 cm/kyr.

At the same time, freshwater influence over the site increased, and the fluvial events at 2.0–2.3, 1.5 (1.2) and < 0.5 cal. ka show a more “contrasting” pattern compared to the older ones (Fig. 6). It should be also mentioned, that there are indications in our records of core PM9482-2 that prior to 2.7 cal. ka more river runoff water flow was directed to the north off the delta (high ASR, high influxes of terrestrial palynomorphs), but then it was reduced. The 1.5 cal. ka and the 1.2 cal. ka events (that could be the same event, see Section 4.1) are the most evident indications of a short-lived fluvial influence as recorded by the rapid rise in ASR to > 700 cm/kyr, abundant inclusions of plant debris and wood fragments, the highest influxes of pollen/spores and chlorophycean algae, increased C/Tsh ratio, and a negative  $\delta^{13}\text{C}$  excursion of about 1‰ (Figs. 4, 6). The reconstructed surface water salinity at the site is below 11–12 psu (Polyakova et al., 2006). This freshwater outflow likely affected also the distant offshore site PS51/92, where sedimentation rates rose to nearly 500 cm/kyr between 1.3 and 1.1 cal. ka (Mueller-Lupp et al., 2004), and surface water salinity dropped to 13–14 psu and less (Polyakova et al., 2006). The freshwater influence over the site initiated a strong reversed inflow of saline open-sea water that resulted in the simultaneous increase in  $\delta^{18}\text{O}$  up to the highest values of > 1‰, the highest proportions of river-intermediate benthic foraminifers (including *C. reniforme*) and shallow-water marine ostracods, and the maximum occurrence of planktic foraminifers. Overall, with increasing water depth the mixing effect decreased, and the water column at the study site became more stratified. Stabilization of the water column structure on the inner LS shelf after 4 ka has been reconstructed from nitrogen isotope data with establishment of modern-like conditions of a strong summer stratification after 2 ka (Thibodeau et al., 2018). The general climate cooling as revealed by the pollen data (see Section 5.1) and water column stabilization probably favoured enhanced sea-ice formation. Together with periodically strong fluvial events this formed suitable habitat conditions for the opportunistic species *E. clavatum*. The enhanced fluvial influence over the study site as expressed by the 1.5 cal. ka event could be also due to the further offshore protrusion of the LR delta and continuing tectonically preconditioned redistribution of the river runoff in the northeastern/eastern direction (Schwamborn et al., 2002a; Polyakova et al., 2006; Korotaev, 2011).

The strongest freshwater influence upon the site PS51/80 in combination with reversed current activity is characteristic for the last 500 years. The extremely negative  $\delta^{13}\text{C}$  values observed during this

time period could be a result of light DIC composition of the bottom water due to re-mineralization of organic matter produced by phytoplankton in response to the input of nutrient-rich LR water (Erlenkeuser, 1995). But it has been shown on the basis of water analyses that the LR water itself has an inherently low  $\delta^{13}\text{C}$  in DIC of approximately  $-7\text{‰}$  (Bauch et al., 2004; Fig. 6). We therefore suppose that the significant change seen in the foraminiferal  $\delta^{13}\text{C}$  during the past 500 years gives evidence for a major diversion of the main LR outflow via its eastern branches (Trofimovskaya and Bykovskaya) and establishment of the modern hydrological delta channel network with > 80% of the runoff going to these two branches.

However, this could also be partly a result of a generally increasing river runoff to the Eurasian Arctic seas. At site PM9482-2, the increase in sedimentation rates during the last 300 years (Fig. 2) and elevated influxes of terrestrial palynomorphs and freshwater green algae during the last 200 years likely resulted from the overall increase in river runoff (probably, in combination with enhanced coastal abrasion). In the inner Kara Sea, a slight decrease in  $\delta^{13}\text{C}$  during the last 2–3 kyr coincides with an elevated content of freshwater diatoms, along with the increasing proportion of marine species *C. reniforme* (Polyak et al., 2002b, 2003), thus highlighting the same pattern of enhanced river runoff combined with reversed bottom currents. A slight increase in magnetic susceptibility in the core close to the Yenisei estuary is observed at 1.5 and 1 cal. ka, although progressive cooling remains the general trend of climate variability during the last 2.5 cal. kyr (Stein et al., 2004).

## 6. Conclusions

Land-shelf interactions and related environmental changes were reconstructed for the past 6 cal. kyr based on multiproxy records from AMS<sup>14</sup>C-dated sediment cores located on the inner LS shelf to the north and northeast of the LR delta.

- The observed changes are determined by the overall mid- to late Holocene climate variability, progressive coastline retreat due to thermoabrasion, and river runoff fluctuations. The latter are climatically preconditioned, but in the study area they also depend on the redistribution of river outflow between river branches within the delta and the offshore protrusion of the delta itself.
- Comparison of the obtained palynomorph records with those available from coastal lakes and across the LR catchment shows that the LR outflow largely determined the composition of species associations and the magnitude of terrestrial matter influx from land.
- Pollen assemblages of the inner LS shelf reflect the mixed environmental signal and complex pollen contribution of the adjacent Arctic tundra and remote taiga zones drained by the LR. These indicate a vegetation response to warmer-than-present climatic conditions between 6 and 4.5 cal. ka and a subsequent gradual cooling.
- Episodes of enhanced freshwater influence in the surface water layer (fluvial events) are manifested in the records by increases in sedimentation rates; high influx of terrestrial material (pollen and spores, freshwater chlorophycean algae, wood and plant remains); negative benthic  $\delta^{13}\text{C}$  values and radiocarbon age reversals due to specific DIC signature of the LR water. They tend to correlate with positive benthic  $\delta^{18}\text{O}$  excursions, increasing representation of river-distal species among benthics and the presence of rare planktic foraminifers. This points to an estuarine-like reversed (north to south) bottom current activity along the submarine paleovalleys.
- The most pronounced fluvial events were recorded at 5.3–5.9, 1.5 (1.2) and < 0.5 cal. ka. The oldest fluvial event coincides with the final phase of the mid-Holocene climate warming. The event at 1.5 (1.2) cal. ka is specifically strong at the northeastern site thus likely marking a direction change of the Lena River outflow at this time and the progressive protrusion of the delta. During the past 500 years distinct negative  $\delta^{13}\text{C}$  values at the northeastern site

reflect enhanced riverine influence. It is therefore concluded that the unprecedented change in the  $\delta^{13}\text{C}$  trend corroborates the other evidence for a principal diversion of the major Lena River outflows into its present-day, easterly direction.

### Declaration of competing interest

The authors declare that they have no known competing financial interests or personal relationships that could have appeared to influence the work reported in this paper.

### Acknowledgements

This research is a contribution to the joint Russian-German research project "Changing Arctic Transpolar System (CATS)": H.A.B. acknowledges financial support of BMBF (project no. 03F0776); E.T. and Ya.O. acknowledge financial support of the Ministry of Science and Higher Education of the Russian Federation (project no. RFMEFI61617X0076).

### Appendix A. Supplementary data

Supplementary data to this article can be found online at <https://doi.org/10.1016/j.palaeo.2019.109502>.

### References

- ACIA, 2005. Arctic Climate Impact Assessment - Scientific Report. Cambridge University Press, Cambridge.
- Alabyan, A.M., Chalov, R.S., Korotaev, V.N., Sidorchuk, A.Y., Zaitsev, A.A., 1995. Natural and technogenic water and sediment supply to the Laptev Sea. *Berichte zur Polarforschung* 176, 265–271.
- Alpat'ev, A.M., Arkhangel'skii, A.M., Podoplelov, N.Y., Stepanov, A.Y., 1976. *Fizicheskaya Geografiya SSSR ('Aziatskaya Chast')* (Physical Geography of the USSR (Asian Part)). Vysshaya Shkola, Moscow (in Russian).
- Andreev, A., Tarasov, P., Schwamborn, G., Ilyashuk, B., Ilyashuk, E., Bobrov, A., Klimanov, V., Rachold, V., Hubberten, H.W., 2004a. Holocene paleoenvironmental records from Nikolay Lake, Lena River Delta, Arctic Russia. *Palaeogeogr., Palaeoclim., Palaeoecol.* 209, 197–217.
- Andreev, A.A., Tarasov, P.E., 2007. Pollen records, postglacial: Northern Asia. In: Elias, S.A. (Ed.), *Encyclopedia of Quaternary Science*. 4. Elsevier, Amsterdam, the Netherlands, pp. 2721–2729.
- Andreev, A.A., Tarasov, P.E., Klimanov, V.A., Melles, M., Lisitsyna, O.M., Hubberten, H.-W., 2004b. Vegetation and climate changes around the Lama Lake, Taymyr Peninsula, Russia during the Late Pleistocene and Holocene. *Quat. Int.* 122, 69–84.
- Andreev, A.A., Schirmermeister, L., Tarasov, P.E., Ganopolski, A., Brovkin, V., Siebert, C., Wetterich, S., Hubberten, H.-W., 2011. Vegetation and climate history in the Laptev Sea region (Arctic Siberia) during Late Quaternary inferred from pollen records. *Quat. Sci. Rev.* 30, 2182–2199.
- Are, F., Reimnitz, E., 2000. An overview of the Lena River Delta setting: geology, tectonics, geomorphology, and hydrology. *J. Coastal Res.* 16 (4), 1083–1093.
- Are, F.E., 1980. Thermal Abrasion of Sea Coasts. Nauka, Moscow (in Russian).
- Atlas Arktiki (Atlas of the Arctic). GUGK, Moscow (in Russian).
- Babalola, L.O., Patterson, R.T., Prokoph, A., 2013. Foraminiferal evidence of a late Holocene westward shift of the Aleutian low pressure system. *J. Foraminiferal Res.* 43 (2), 127–142.
- Bauch, H.A., Polyakova, Y., 2000. Late Holocene variations in Arctic shelf hydrology and sea-ice regime: evidence from north of Lena Delta. *Int. J. Earth Sci.* 89 (3), 569–577.
- Bauch, H.A., Kassens, H., Erlenkeuser, H., Grootes, P.M., Thiede, J., 1999. Depositional environment of the Laptev Sea (Arctic Siberia) during the Holocene. *Boreas* 28, 194–204.
- Bauch, H.A., Kassens, H., Kunz-Pirrung, M., Naidina, O., Thiede, J., 2001a. Composition and flux of Holocene sediments on the eastern Laptev Sea shelf. *Arctic Siberia. Quat. Res.* 55, 344–351.
- Bauch, H.A., Mueller-Lupp, T., Taldenkova, E., Spielhagen, R.F., Kassens, H., Grootes, P.M., Thiede, J., Heinemeier, J., Petryashov, V.V., 2001b. Chronology of the Holocene transgression at the North Siberian margin. *Glob. Planet. Change* 31, 125–139.
- Bauch, H.A., Erlenkeuser, H., Bauch, D., Mueller-Lupp, T., Taldenkova, E., 2004. Stable oxygen and carbon isotopes in modern foraminifera from the Laptev Sea shelf: implications for reconstructing proglacial and profluvial environments in the Arctic. *Mar. Micropal.* 51, 285–300.
- CAVM Team, 2003. Circumpolar Arctic Vegetation Map, Scale 1:7,500,000. Conservation of Arctic Flora and Fauna (CAFF) Map no.1. U.S. Fish and Wildlife Service, Anchorage, Alaska. <http://www.geobotany.uaf.edu/cavm/finalcavm/index.html>.
- De Vernal, A., Henry, M., Matthiessen, J., Mudie, P.J., Rochon, A., Boessenkool, K.P., Eynaud, F., Grosfeld, K., Guiot, J., Hamel, D., Harland, R., Head, M.J., Kunz-Pirrung, M., Levac, E., Loucheur, V., Peyron, O., Pospelova, V., Radi, T., Turon, J.-L., Voronina, E., 2001. Dinoflagellate cyst assemblages as tracers of sea-surface conditions in the northern North Atlantic, Arctic and sub-Arctic seas: the new 'n = 677' data base and its application for quantitative paleoceanographic reconstruction. *J. Quat. Sci.* 16, 681–698.
- Dmitrenko, I.A., Hoeselmann, J.A., Kirillov, S.A., Wegner, C., Gribanov, V.A., Berezovskaya, S.L., Kassens, H., 2001a. Thermal regime of the Laptev Sea bottom layer and affecting processes. *Earth's Cryosphere* 5 (3), 40–55.
- Dmitrenko, I.A., Hoeselmann, J.A., Kirillov, S.A., Berezovskaya, S.L., Kassens, H., 2001b. Role of barotropic sea level changes in current formation on the eastern shelf of the Laptev Sea. *Dokl. Earth Sci.* 377 (2), 243–249.
- Erlenkeuser, H., 1995. TRANSDRIFT II Shipboard Scientific Party. Stable carbon isotope ratios in the waters of the Laptev Sea/Sept. 94. *Berichte zur Polarforschung* 176, 170–177.
- Fatela, F., Taborda, R., 2002. Confidence limits of species proportions in microfossil assemblages. *Mar. Micropal.* 45, 169–174.
- Frenzel, P., Keyser, D., Viehberg, F.A., 2010. An illustrated key and (palaeo) ecological primer for postglacial to recent Ostracoda (Crustacea) of the Baltic Sea. *Boreas* 39, 567–575.
- Gordeev, V.V., Martin, J.M., Sidorov, I.S., Sidorova, M.V., 1996. A reassessment of the Eurasian river input of water, sediment, major elements, and nutrients to the Arctic Ocean. *Amer. J. Sci.* 296, 664–691.
- Grimm, E.C., 1993. TILIA 2.0 Version b.4 (Computer Software). Illinois State Museum, Research and Collections Center, Springfield.
- Grimm, E.C., 2004. TGView. Illinois State Museum, Research and Collections Center, Springfield.
- Gusev, E.A., Anikina, N.Y., Derevyanko, L.G., Klyuvitkina, T.S., Polyak, L.V., Polyakova, E.I., Rekant, P.V., Stepanova, A.Yu., 2014. Environmental evolution of the southern Chukchi Sea in the Holocene. *Oceanology* 54 (4), 465–477.
- Hayek, L.-A.C., Buzas, M.A., 1997. *Surveying Natural Populations*. Columbia University Press, New York.
- Holmes, M.L., Creager, J.S., 1974. Holocene history of the Laptev Sea continental shelf. In: Herman, Y. (Ed.), *Arctic Ocean Sediments, Microfauna, and Climatic Record in the Late Cenozoic Time*. Springer-Verlag, New York, pp. 211–229.
- Ivanov, V.V., Piskun, A.A., 1999. Distribution of river water and suspended sediment loads in the deltas of rivers in the Laptev Sea and east-Siberian Seas. In: Kassens, H., Bauch, H.A., Dmitrenko, I., Eicken, H., Hubberten, H.-W., Melles, M., Thiede, J., Timokhov, L. (Eds.), *Land-ocean Systems in the Siberian Arctic: Dynamics and History*. Springer, Berlin Heidelberg New-York, pp. 239–250.
- Kapper, O.G., 1954. *Khvoynnye porody (Conifers)*. Goslesbumizdat, Moscow-Leningrad, pp. 304 (in Russian).
- Kassens, H., Dmitrenko, I., 1995. The Transdrift II expedition to the Laptev Sea. In: Kassens H. (Ed.) *Laptev Sea System: expeditions in 1994*. Reports on Polar Research 182, 1–180.
- Kassens, H., Dmitrenko, I.A., Rachold, V., Thiede, J., Timokhov, L., 1998. Russian and German scientists explore the Arctic's Laptev Sea and its climate system. *EOS Transaction American Geophysical Union* 79, 317–323.
- Kassens, H., Lisitsin, A.P., Thiede, J., Polyakova, Y.I., Timokhov, L.A., Frolov, I.E. (Eds.), 2009. *Sistema morya Laptevyykh i priliegayushchikh arkticheskikh morei: sovremennyye usloviya i paleoklimat (The system of the Laptev Sea and adjacent Arctic Seas: Current status and history of development)*. Moscow State University, Moscow, pp. 1–608 (in Russian).
- Kerwin, M., Overpeck, J.T., Webb, R.S., De Vernal, A., Rind, D.H., Healy, R.J., 1999. The role of oceanic forcing in mid-Holocene northern hemisphere climatic change. *Palaeogeography* 14, 200–210.
- Kim, So-Y., Polyak, L., Delusina, I., Delusina, I., 2016. Terrestrial and aquatic palynomorphs in Holocene sediments from the Chukchi-Alaskan margin, western Arctic Ocean: Implications for the history of marine circulation and climatic environments. *The Holocene* 27 (7), 976–986. <https://doi.org/10.1177/0959683616678459>.
- Kleiber, H.P., Niessen, F., 1999. Late Pleistocene paleoriver channels on the Laptev Sea Shelf - implications from sub-bottom profiling. In: Kassens, H., Bauch, H.A., Dmitrenko, I., Eicken, H., Hubberten, H.-W., Melles, M., Thiede, J., Timokhov, L. (Eds.), *Land-ocean Systems in the Siberian Arctic: Dynamics and History*. Springer-Verlag, New York, pp. 635–656.
- Klyuev, E.V., Kotyukh, A.A., Olenina, N.V., 1981. Cartographical-hydrographical interpretation of the disappearance of icelands Semenovskii and Vasil'evskii in the Laptev Sea. *Izvestiya Vsesoyuznogo geographicheskogo obshchestva (Journal of All-Union Geographical Society)* 6, 485–492 (in Russian).
- Klyuvitkina, T.S., Bauch, H.A., 2006. Hydrological changes in the Laptev Sea during the Holocene inferred from the studies of aquatic palynomorphs. *Oceanology* 46 (6), 859–868.
- Komárek, J., Jankovská, V., 2001. Review of the green algal genus *Pediastrum*: Implication for pollenanalytical research. *Bibl. Phycol.* 108, 1–127.
- Korotaev, V.N., 1984. The formation of the hydrographic network of the Lena Delta in the Holocene. *Vestnik MGU, ser. 5 geography*. 6, 39–44 (in Russian).
- Korotaev, V.N., 2011. Holocene history of river deltas of the Siberian Arctic coast. *Geografiya i prirodnye resursy (Geography and natural resources)* 3, 13–20 (in Russian).
- Kunz-Pirrung, M., 1998. Aquatic palynomorphs: reconstruction of Holocene sea surface water masses in the eastern Laptev Sea. *Berichte zur Polarforschung* 281.
- Kupriyanova, L.A., Aleshina, L.A., 1978. *Pyltsa Dvudolnykh Flory Evropeiskoi Chasti SSSR (Pollen of Dicotyledons from the Flora of the European Part of the USSR)*. Nauka, Leningrad (in Russian).
- MacDonald, G.M., Velichko, A.A., Kremetski, C.V., Borisova, O.K., Goleva, A.A., Andreev, A.A., Cwynar, L.C., Riding, R.T., Forman, S.L., Edwards, T.W.D., Aravena, R., Hammarlund, D., Szeicz, J.M., Gattaulin, V.N., 2000. Holocene treeline history and climate change across Northern Eurasia. *Quat. Res.* 53, 302–311.
- Matthiessen, J., 1995. Distribution patterns of dinoflagellate cysts and other organic-

- walled microfossils in recent Norwegian-Greenland Sea sediments. *Mar. Micropal.* 24, 307–334.
- Matthiessen, J., Kunz-Pirrung, M., Mudie, P.J., 2000. Freshwater chlorophycean algae in recent marine sediments of the Beaufort, Laptev and Kara Seas (Arctic Ocean) as indicators of river runoff. *Intern. J. Earth Sci.* 89, 470–485.
- Alekseev, G.V. (Ed.), 2011. *Meteorologicheskii i Geofizicheskiye Issledovaniya* (Meteorological and Geophysical Researches). SPb., Paulsen Publ, Moscow (in Russian).
- Meyer, H., Opel, T., Laepple, T., Meyer, H., Opel, T., Laepple, T., 2015. Long-term winter warming trend in the Siberian Arctic during the mid- to late Holocene. *Nature Geoscience Letters*. <https://doi.org/10.1038/NGEO2349>. Published online.
- Monserud, R.A., Tchekakova, N.M., Denissenko, O.V., 1998. Reconstruction of the mid-Holocene paleoclimate of Siberia using a bioclimatic vegetation model. *Palaeogeogr., Palaeoclim., Palaeoecol.* 139, 15–36.
- Mueller-Lupp, T., Bauch, H.A., Erlenkeuser, H., 2004. Holocene hydrographical changes of the eastern Laptev Sea (Siberian Arctic) recorded in  $\delta^{18}\text{O}$  profiles of bivalve shells. *Quat. Res.* 61, 32–41.
- Müller, S., Tarasov, P.E., Andreev, A.A., Tütken, T., Gartz, S., Diekmann, B., Müller, S., Tarasov, P.E., Andreev, A.A., Tütken, T., Gartz, S., Diekmann, B., 2010. Late Quaternary vegetation and environments in the Verkhoyansk Mountains region (NE Asia) reconstructed from a 50-kyr fossil pollen record from Lake Billyakh. *Quat. Sci. Rev.* 29, 2071–2086.
- Müller, S., Tarasov, P.E., Diekmann, B., Andreev, A.A., 2009. Late Glacial to Holocene environments in the present-day coldest region of the Northern Hemisphere inferred from a pollen record of Lake Billyakh, Verkhoyansk Mts, NE Siberia. *Clim. of the Past* 5, 73–84.
- Naidina, O.D., Bauch, H.A., 2001. A Holocene pollen record from the Laptev Sea shelf, Northern Yakutia. *Glob. Planet. Change* 31, 141–153.
- Naidina, O.D., Bauch, H.A., 2011. Early to middle Holocene pollen record from the Laptev Sea (Arctic Siberia). *Quat. Int.* 229, 84–88.
- Opel, T., Dereviagin, A.Yu, Meyer, H., Meyer, H., Schirmer, L., Wetterich, S., 2011. 905 Palaeoclimatic information from stable water isotopes of Holocene ice wedges on the Dmitrii 906 Laptev Strait, northeast Siberia, Russia. *Permafrost. Periglac. Process.* 22, 84–100.
- Overpeck, J., Huguén, K., Hardy, R., Bradley, R., Case, R., Douglas, M., Finney, B., Gajewski, K., Jacoby, G., Gennings, A., Lamoureux, S., Lasca, A., MacDonald, G., Moore, J., Retelle, M., Smith, S., Wolfe, A., Zielinski, G., 1997. Arctic environmental change of the last four centuries. *Science* 278 (14), 1251–1256.
- Ovsepyan, Y., 2016. Late Quaternary Laptev Sea Foraminifera and Environmental Reconstructions Based on Palaeoecology Proxy. PhD Thesis. GIN RAS, Moscow (in Russian).
- Patterson, R.T., Kumar, A., 2002. Post-glacial palaeoceanographic history of Saanich inlet, British Columbia, based on foraminiferal proxy data. *J. Foraminiferal Res.* 32 (2), 110–125.
- Perfil'eva, V.I., Teterina, L.V., Karpov, N.S., 1991. Rastitel'nyi Pokrov tundrovoy zony Yakutii (Vegetation cover of the tundra zone of Yakutia). In: Yakutsk, 1991, (in Russian).
- Peterson, B.J., Holmes, R.M., McClelland, J.M., Charles, J., Vörösmarty, C.J., Lammers, R.B., Shiklomanov, A.I., Shiklomanov, I.A., Rahmstorf, S., 2002. Increasing river discharge to the Arctic Ocean. *Science* 298 (5601), 2171–2173.
- Pisarcic, M.F.J., MacDonald, G.M., Velichko, A.A., Cwynar, L.C., 2001. The Lateglacial and postglacial vegetation history of the northwestern limits of Beringia, based on pollen, stomate and tree stump evidence. *Quat. Sci. Rev.* 20, 235–245.
- Pivovarov, S., Hölemann, J.A., Kassens, H., Piepenburg, D., Schmid, M.K., 2005. Laptev and East Siberian seas (23, P). In: Robinson, A.R., Brink, K.H. (Eds.), *The Sea*. 14. Harvard University Press, pp. 1111–1137 Chapter 28.
- Polyak, L., Korsun, S., Febo, L., Stanovoy, V., Khusid, T., Hald, M., Paulsen, B.E., Lubinski, D.A., 2002a. Benthic foraminiferal assemblages from the southern Kara Sea, a river-influenced Arctic marine environment. *J. Foraminiferal Res.* 32 (3), 252–273.
- Polyak, L., Levitan, M., Khusid, T., Merklin, L., Mukhina, V., 2002b. Variations in the influence of riverine discharge on the Kara Sea during the last deglaciation and the Holocene. *Glob. Planet. Change* 32, 291–309.
- Polyak, L., Stanovoy, V., Lubinski, D.J., 2003. Stable isotopes in benthic foraminiferal calcite from a river-influenced Arctic marine environment, Kara and Pechora Seas. *Paleoceanography* 18 (1), 1003. <https://doi.org/10.1029/2001PA000752>. (2003).
- Polyakova, Ye.I., Bauch, H.A., Klyuvitkina, T.S., 2005. Early to middle Holocene changes in Laptev Sea water masses deduced from diatom and aquatic palynomorph assemblages. *Glob. Planet. Change* 48, 208–222.
- Polyakova, Y., Klyuvitkina, T.S., Novichkova, E.A., Bauch, H.A., Kassens, H., 2006. High-resolution reconstruction of Lena River discharge during the Late Holocene inferred from microalgal assemblages. *Polarforschung* 75 (2–3), 83–90.
- Polyakova, Y., Klyuvitkina, T.S., Novichkova, E.A., Bauch, H.A., Kassens, H., 2009. Changes in the Lena River runoff during the Holocene. *Water Resources* 36 (3), 273–283.
- Rachold, V., Grigoriev, M.N., Are, F.E., Solomon, S., Reimnitz, E., Kassens, H., Antonow, M., 2000. Coastal erosion vs riverine sediment discharge in the Arctic Shelf seas. *Int. J. Earth Sci.* 89, 450–460.
- Razina, V.V., Polyakova, Ye.I., Kassens, H., Bauch, H.A., 2007. Evolution of the Postglacial Vegetation in the Western Laptev Sea Region (Siberian Arctic). *Polarforschung* 76 (3), 125–132.
- Reille, M., 1992. Pollen et spores d'Europe et d'Afrique du nord. *Laboratoire de Botanique Historique et Palynologie, Marseille*.
- Rivera, J., Karabanov, E.B., Douglas, F., Williams, D.F., Buchinsky, V., Kuzmin, M., 2006. Lena River discharge events in sediments of Laptev Sea, Russian Arctic. *Estuar. Coast. Shelf Sci.* 66, 185–196.
- Rudenko, O., Tarasov, P.E., Bauch, H.A., Taldenkova, E., 2014. A Holocene palynological record from the northeastern Laptev Sea and its implications for palaeoenvironmental research. *Quat. Int.* 348, 82–92.
- Rudenko, O.V., Yenina, V.V., Ovsepyan, Y., 2015. Variations in the composition of sub-fossil pollen spectra from bottom sediments of the shelf and continental slope of the Laptev Sea. In: *Proceed. of XXI Intern. School of Mar. Geology*. v.1. GEOS, Moscow, pp. 218–221 (in Russian).
- Savelieva, L.A., Raschke, E.A., Titova, D.V., 2013. Atlas Fotografii Rastenii i Pylytsy Dely Reki Leny (Photographic Atlas of Plants and Pollen of the Lena River Delta). SPbGU, Saint-Petersburg (in Russian).
- Schwamborn, G., Rachold, V., Grigoriev, M.N., 2002a. Late Quaternary sedimentation history of the Lena Delta. *Quat. Int.* 89, 119–134.
- Schwamborn, G., Andreev, A.A., Rachold, V., Hubberten, H.-W., Grigoriev, M.N., Tumskey, V., Pavlova, E.Y., Dorozhkina, M.V., 2002b. Evolution of Lake Nikolay, Arga Island, western Lena River delta, during late Pleistocene and Holocene time: the modern and ancient terrestrial and coastal environment of the Laptev Sea region, Siberian Arctic. *Polarforschung* 70, 69–82.
- Sokolovskaya, A.P., 1955. Pollen of Arctic plants. In: *Nauchnyi Byulleten*. 33. LGU, Leningrad, pp. 244–292 (in Russian).
- Sokolov, S.Ya., Svyazeva, O.F., Kubli, V.A., 1977. Arealy derev'ev i kustarnikov SSSR (Areas of the trees and shrubs of the USSR). In: *Nauka Publ. House*, pp. 164 Leningrad. USSR. V. 1. 164 (in Russian).
- Stein, R., Dittmers, K., Fahl, K., Kraus, M., Matthiessen, J., Niessen, F., Pirrung, M., Polyakova, Ye, Schoster, F., Steinke, T., Fuetterer, D.K., 2004. Arctic (palaeo) river discharge and environmental change: evidence from the Holocene Kara Sea sedimentary record. *Quat. Sci. Rev.* 23, 1485–1511.
- Stepanova, A., Taldenkova, E., Bauch, H.A., 2003. Recent Ostracoda of the Laptev Sea (Arctic Siberia): taxonomic composition and some environmental implications. *Mar. Micropal.* 48 (1–2), 23–48.
- Stepanova, A., Taldenkova, E., Simstich, J., Bauch, H.A., 2007. Comparison study of the modern ostracod associations in the Kara and Laptev seas: Ecological aspects. *Mar. Micropal.* 63, 111–142.
- Stockmarr, J., 1971. Tablets spores used in absolute pollen analysis. *Pollen Spores* 13, 616–621.
- Stone, T.A., Schlesinger, P., 1993. Digitization of the Map "Vegetation of the Soviet Union, 1990". A Report to the Northeastern Forest Experiment Station. USDA Forest Service, Global Change Research Program, Radnor, Pennsylvania.
- Stuiver, M., Reimer, P.J., Reimer, R.W., 2017. CALIB 7.1. [WWW program] at. <http://calib.org>. Accessed date: 22 October 2017.
- Taldenkova, E., Bauch, H.A., Stepanova, A., Dem'yankov, S., Ovsepyan, A., 2005. Last postglacial environmental evolution of the Laptev Sea shelf as reflected in molluscan, ostracod and foraminiferal faunas. *Glob. Planet. Change* 48 (1–3), 223–251.
- Taldenkova, E., Bauch, H.A., Stepanova, A., Strezh, A., Dem'yankov, S., Ovsepyan, Y., 2008. Postglacial to Holocene history of the Laptev Sea continental margin: Palaeoenvironmental implications of benthic assemblages. *Quat. Int.* 183, 40–60.
- Thibodeau, B., Bauch, H.A., Knies, J., 2018. Impact of Arctic shelf summer stratification on Holocene climate variability. *Quat. Sci. Rev.* 191, 229–237.
- Velichko, A.A., Andreev, A.A., Klimanov, V.A., 1997. Climate and vegetation dynamics in the tundra and forest zone during the late glacial and Holocene. *Quat. Int.* 41–42, 71–96.
- Wagner, A., Lohmann, G., Prange, M., 2011. Arctic river discharge trends since 7 ka BP. *Glob. Planet. Change* 79, 48–60.
- Wegner, C., Hölemann, J.A., Kirillov, S., Tuschling, K., Abramova, E., Kassens, H., 2003. Suspended particulate matter on the Laptev Sea shelf (Siberian Arctic) during ice-free conditions. *Estuar. Coast. Shelf Sci.* 57, 55–65.
- Wegner, C., Hölemann, J.A., Dmitrenko, I., Kirillov, S., Kassens, H., 2005. Seasonal variations in Arctic sediment dynamics – evidence from 1-year records in the Laptev Sea (Siberian Arctic). *Glob. Planet. Change* 48, 126–140.
- Whatley, R., 1983. Some simple procedures for enhancing the use of Ostracoda in palaeoenvironmental analysis. *Norw. Petrol. Direct. Bull.* 2, 129–146.
- Wolfe, B.B., Edwards, T.W.D., Aravena, R., Forman, S.L., Warner, B.G., Velichko, A.A., MacDonald, G.M., 2000. Holocene palaeohydrology and palaeoclimate at treeline, north-central Russia, inferred from oxygen isotope records in lake sediment cellulose. *Quat. Res.* 53, 319–329.